EUROPEAN COMMISSION

Community research

BELBaR

(Contract Number: 295487)

WP3 partners final report on experimental results on micro- to macroscale colloid rock interaction and colloid radionuclide interaction

DELIVERABLE (D-N°:3.11)

T. Schäfer (editor)

Author:

N. Sherriff, N. Bryan, F Livens (UNIMANCH)
M. Bouby, G. Darbha, M. Stoll, F. Huber, T. Schäfer (KIT-INE)
P. Hölttä, O. Elo, V. Suorsa, E. Honkaniemi, S. Niemiaho
T. Missana, U. Alonso, N. Mayordomo (CIEMAT)
K. Kolomá, R. Červinka (ÚJV Řež, a. s.)
A. Y. Romanchuk, , P.K. Verma, V.G. Petrov, S.N. Kalmykov (MSU)

Reporting period: e.g. 01/03/12 – 31/12/15

Date of issue of this report: **29/02/16**

Start date of project: **01/03/12** Duration: 48 Months

EURATOM

DISTRIBUTION LIST

Name	Number of copies	Comments
Christophe Davies (EC) BELBaR participants		

Project co-funded by the European Commission under the Seventh Euratom Framework Programme for Nuclear Research &Training Activities (2007-2011)		
Dissemination Level		
PU	Public	

Table of content

1.0 Introduction

In WP3 of the collaborative project BELBaR in total six partners (CIEMAT, MSU, HU, UNIMANCH, UJV and KIT) investigated colloid mobility controlling processes in the geosphere and the effect of the mobile colloidal phase on the transport of radionuclides in the far-field environment of a deep geological repository in crystalline formations *(i.e. granite from Grimsel; Switzerland, Äspö; Sweden, Kuru gray granite and Olkiluoto tonalite; Finland, Melechov massif (depth 97.5-98.7 m); Czech Republic and Russia)*. The inorganic colloidal phase investigated consists mainly of montmorillonite, but in the process oriented investigations also synthetic phases as engineered nanoparticles (e.g. gold colloids) or polystyrene nano-spheres have been used to gain insides into retention processes. The investigations within WP3 focussed on one hand side on microscale investigations and on the other hand side on macroscale investigations including work in near-natural systems. Another main focus of WP3 was on the process understanding of radionuclide colloid interaction with a special emphasis on sorption reversibility. Finally, all the information gained within the project, but also outside the consortium is planned to feed into a mechanistic model of the colloid radionuclide interaction. This model is described in detail in D3.10 and will not discussed in detail in this document.
From the structure of the project the source term concerning colloid concentration generated via erosion and the size distribution of colloidal material released from the compacted bentonite is documented in the WP2 final report and gives an upper bound limit of the colloid concentration to be expected under glacial melt water conditions. This concentration and size distribution of colloidal material is a function of the geochemical conditions, i.e. pH, ionic strength, porewater composition and presence/absence of organic material. A huge data screening has been performed in WP 4 concerning the stability of colloidal phases including modelling activities which are documented in the WP 4 final report. The overarching structure is schematically presented in Figure 1 and a generic graphical abstract presented in Figure 2.

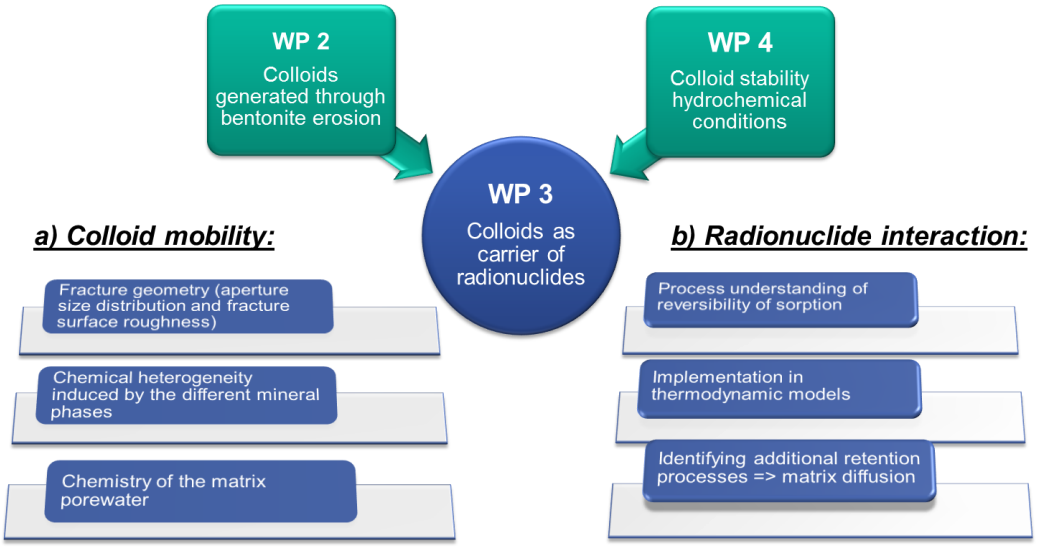

Figure 1: ***Objectives of WP3 in the BELBaR project***

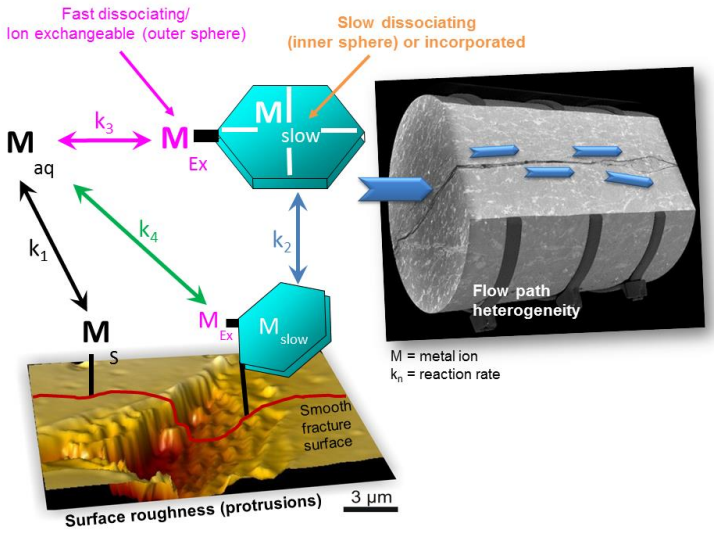

Figure 2: ***Generic graph of the processes investigated in WP3***

From waste management perspective and safety case position there are three issues tackled in WP 3 of CP BELBaR with assumptions made concerning the issue of colloids and colloid-mediated radionuclide transport (see table 1).

Table 1: ***Issues concerning WP3 to be discussed as an input for WP1 (Consideration of Colloids in the Safety Case)***

Issue	**Safety case position at start of BELBaR**	**Outcomes for final State-of-art report**
Colloid mobility controlling processes	• Clay colloids have not been considered radionuclide carriers due to the assumed low contribution. • Rather than attempting to develop detailed process models for colloid-facilitated transport, potential mitigating processes are ignored so as to place an upper bound on the possible effect.	Validation or invalidation of this assumption (WP3). Is there an upper bound for colloid-mediated transport?
Retention processes	• Retardation of colloid transport in the far field, will delay the arrival of radionuclides in the biosphere. • The extent of this isn't currently taken into account.	Safety arguments to support retardation mechanisms (WP3).
Radionuclide sorption	To assess the possible role of rapid reversible sorption/ desorption onto colloids in facilitating transport, the following assumptions have been adopted: 1. equilibrium sorption of radionuclides onto mobile and immobile colloids, 2. equilibrium sorption of colloids onto fracture surfaces, and 3. colloid- free matrix pore space (conservative assumption, but also realistic for the small pore sizes of granitic rock). Reversible, linear sorption of radionuclides onto colloids has been assumed.	Is the assumption of reversible, linear sorption of radionuclides onto colloids justified? (WP3)

2.0 Colloid mobility controlling processes and retention

In fractured rocks, colloid transport mainly takes place by advection in the water flow, being greatly affected by different mechanisms that contribute to colloid filtration. Colloid contribution to radionuclide (RN) transport is subjected to the joint compliance of several conditions (Miller et al., 1994), including colloid existence, stability and mobility (e.g. the "colloidal ladder").

2.1 Microscale and macroscale colloid retention studies (CIEMAT)

Colloid retention has been observed even at conditions where high retention was not expected, i.e. under unfavourable electrostatic conditions (Missana et al., 2008a; Schäfer et al., 2004). Colloid erosion and mobility was also analysed in-situ at the FEBEX tunnel at the Grimsel Test Site (Switzerland) (Missana et al, 2015a). The mechanisms that contribute to colloid retention are not yet fully understood (Geckeis et al, 2008; Missana et al, 2008a; Albarran et al, 2011; Missana et al, 2011; Schäfer et al, 2012).
Colloid diffusion in rock matrix can eliminate colloids from the flow paths and, despite being considered a minor mechanism, it is often accounted for to interpret the tailing behaviour of colloid breakthrough curves in transport experiments (James and Chrysikopoulos, 1999). However, it has been shown that the complex fracture geometry has the same influence on the tailing of the breakthrough curve and based on the missing chromatography effect for colloids observed it is argued that matrix diffusion is of minor importance for colloid retention (Kosakowski, 2004; Möri et al., 2003).

In CIEMAT, several laboratory experiments with bentonite colloid (and radionuclides) were carried out, trying to elucidate the main important parameters affecting their transport in crystalline rock fractures. Furthermore, the mobility of colloids was also studied under natural realistic conditions at the Grimsel Test Site (GTS), in the Febex tunnel (Missana et al, 2015a). In parallel, mechanistic sorption studies of different types of radionuclides on bentonite colloids were conducted.

The chemical conditions span from those of the GTS (dilute and alkaline waters) to those of Äspö (significantly more saline). The chemistry of the groundwater/clay system plays an important role on the erosion of the bentonite, on the stability and mobility of generated colloids and also on the adsorption of the contaminant at the colloid surface. On the other hand, water flow and flow paths are decisive on colloid transport. Indeed, hydrodynamic and chemistry are always strictly related. Filtration of bentonite colloids in crystalline fractures was always observed below a threshold limit of the water flow rate (or residence time) (Albarran et al. 2013). This threshold is somewhat colloid and groundwater chemistry dependent.

Figure 3 draws an example of this important point, showing the bentonite colloid recovery under different experimental conditions. The left part of Figure 3 shows the elution curves of bentonite colloids at the same flaw rate (approx. $6 \cdot 10^{-6}$ m/s) and solution ionic strength. In one case (black points), $5 \cdot 10^{-4}$ M of Ca was present in solution. Such a relatively small difference caused a large difference on the colloid elution behavior. The elution in the Na system was 100%, but only 20 % in the Ca-Na electrolyte. In the left part, it can be seen that performing the experiment in Äspö water, the recovery decreased further to values less than

5%. Furthermore, the recovery is strictly dependent on the water flow rate (even in the pure Na-electrolyte) and lower recoveries are then expected under repository conditions. High filtration of colloids in the fractures, will indeed affect the transport of adsorbed radionuclides.

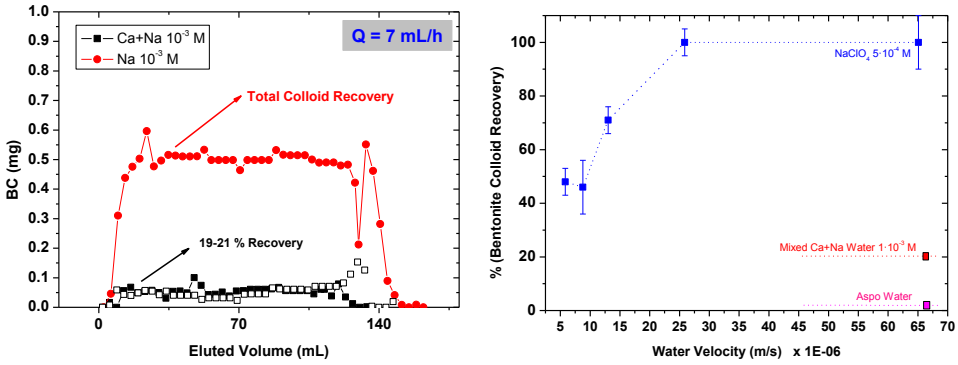

Figure 3: ***Comparison of bentonite colloid recovery under different chemical conditions.***

However, it is important remarking that the mobile fraction of bentonite colloids always moved un-retarded with respect to the water. The fate of the radionuclides will be dependent on the clay/radionuclide interactions especially the reversibility of the adsorption process.

Under dynamic conditions, in most cases, desorption of the radionuclide was observed from the bentonite colloids. Nevertheless, the radionuclide breakthrough curves in the presence of bentonite colloids presented, in certain cases, substantial differences from those in which colloids were not present (Albarran et al., 2011). Figure 4 shows the comparison of Cs transport experiments in granite fractures under Grimsel or Äspo conditions, using similar water flow rates. 100 ppm of bentonite colloids in which Cs ([Cs]=$1 \cdot 10^{-7}$ M) was previously adsorbed (80 % in the Grimsel case and 20 % in the Äspö case) and suspended in synthetic waters representative of the two different cases. The eluted water was analysed to measure Cs activity and the presence of bentonite colloids by photon correlation spectrometry (PCS) in the same samples and to obtain simultaneously colloid and Cs breakthrough curves. The breakthrough curve of Cs, without colloids, presented a single peak with a retardation factor (R_f) of ~200 in the Grimsel case and of ~170 in the Äspö case.

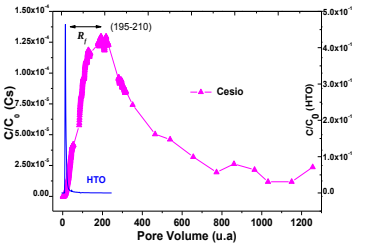

Cs and HTO: without bentonite colloids in Grimsel Water

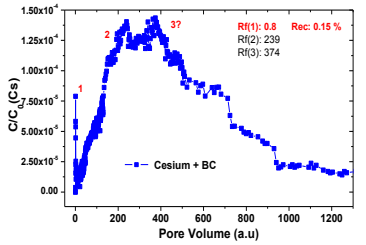

Cs: in the presence of bentonite colloids in Grimsel Water

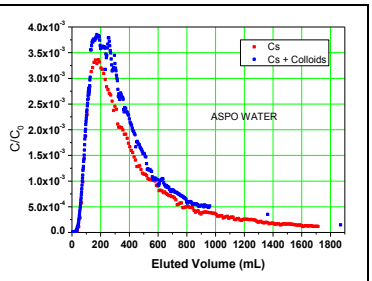

Cs: with and without of bentonite colloids in Aspo Water

Figure 4: ***Examples of transport experiments in fracture with Cs with and without bentonite colloids.***

In the Grimsel case, Cs transport was significantly different in the presence or absence of colloids, whereas the Cs breakthrough curves were more similar in the Äspö case. In the presence of bentonite colloids, in the Grimsel case, the breakthrough curve clearly showed a

small Cs peak in a position very similar to that of the conservative tracer (HTO), with an R_f of 0.8, coincident with the colloid breakthrough peak measured by PCS. The quantity of Cs recovered after this peak was only the 0.15 % of the injected.

Other two peaks were observed in the breakthrough curve with R_f of 200 and 370 approximately. In the Äspö case, no elution of colloids was seen at all, which was not surprising considering that they aggregate fast, under the Äspö water conditions, and can be completely retained in the fracture. Cs, however, eluted. The "split" of the main Cs peak in two peaks with R_f of approximately 170 and 270 was also clearly observed. The appearance of new peaks with retardation factors higher than those showed in the same system without colloids, is most probably due to the modification of the sorption properties of the fracture surface caused by bentonite colloid deposition (Albarran et al., 2013).

Filtration of bentonite colloids (above all at low water flow rates) and their deposition modifies the sorption properties of the granite fracture surface. In most of the cases, the presence of bentonite colloids did not significantly enhance radionuclide transport in the medium, but rather produced a slight increase in the overall retardation in the fracture. Only in the case of very highly sorbing radionuclides like Eu, for which elution was not expected, small elution (less then 7% of the initially adsorbed) was observed and clearly attributable to the presence of the mobile colloidal particles.

CIEMAT also studied micro-scale retention of colloids in granite surface, considering the contribution of access in-depth (diffusion) within the heterogeneous granite surface. Surface retention coefficients were previously analysed in (Alonso et al, 2009).
Micro-scale retention was analysed at mineral scale. In previous work the effect of colloid size on their retention was analysed (Alonso et al. 2007). Within BELBAR project, the effect of the heterogeneous electrostatic charge distribution of granite was deeply analysed.
The selected granite was Aare type from the FEBEX tunnel at the Grimsel Test Site Underground Laboratory (Switzerland) (Huertas et al, 2000). Samples used for diffusion studies have an average area of 1 cm^2 and an average accessible porosity of 0.75 %. Quartz minerals and feldspars showed porosity of 0.5 % while the dark minerals (generally micas and Fe-minerals), which represents about an 8% in volume of the total granite, had higher porosity (> 1.4 %) (Leskinen et al, 2007).

The selected colloids were CeO_2, Fe_2O_3 and Au, with different particle size and charge conditions, diluted in granitic water of low ionic strength (Na-HCO_3 type, pH 8.3 and conductivity 282 µS/cm). The size, stability and charge conditions of the selected colloids and the charge of granite minerals were verified to establish the experimental conditions, accounting for all possible electrostatic interactions. Figure 3 shows the zeta potential measured as a function of pH for studied colloid and for main minerals composing granite, prepared in low mineralized granitic water as a function of pH. At all the pHs, the granite surface charge is, in average, negative. The major minerals composing the granite, as quartz-plagioclases or feldspars (70 % of the total granite) present similar negative behaviour as the granite. However, dark minerals such as biotite, or ilmenite are positively charged at acidic conditions. With this information, the experimental conditions for diffusion analyses were fixed. On the rock part, at acid pH conditions minerals with positive and negative charge coexisted, at acid-neutral conditions minerals showed neutral or negative charge and at basic

conditions most granite minerals are negatively charged. From the colloids, the evaluated cases were: (i) zero charge (Au at pH 3), (ii) low positive charge (CeO_2 and Fe_2O_3 at pH 4-5) (iii) high positive charge (Fe_2O_3 at pH 3, (iv) low negative charge (CeO_2 at pH 10) and (v) high negative charge (Au at pH 6). A summary of studied conditions is presented in Table 2.
For diffusion studies, granite slices, are immersed in the different colloid suspensions and at different pH conditions, during contact times from 5 minutes to 4 days. The granite surfaces were analyzed with Rutherford Backscattering Spectrometry (RBS). As described in (Alonso et al., 2007), where the diffusion of Au colloids of different size (from 2 nm to 250 nm) was analyzed on a Spanish granite.
As example, Figure 5 shows the RBS spectra of granite minerals (biotite and quartz) after contact with CeO_2 colloids at pH 3. At this pH 3, quartz minerals are negatively charged while biotite positively charged (Figure 4). In all the RBS spectra obtained, the signal of Ce is clearly visible being the Ce peaks asymmetrical, presenting a tail pointing towards lower energies indicating that Ce colloids are penetrating in the granite. However, diffusion length was longer in quartz or feldspar minerals due to attractive interaction.
The same analyses were carried out in all considered cases, and in order to obtain diffusion lengths and diffusion coefficients on selected minerals spectra simulation was carried out as described in (Alonso et al, 2007).

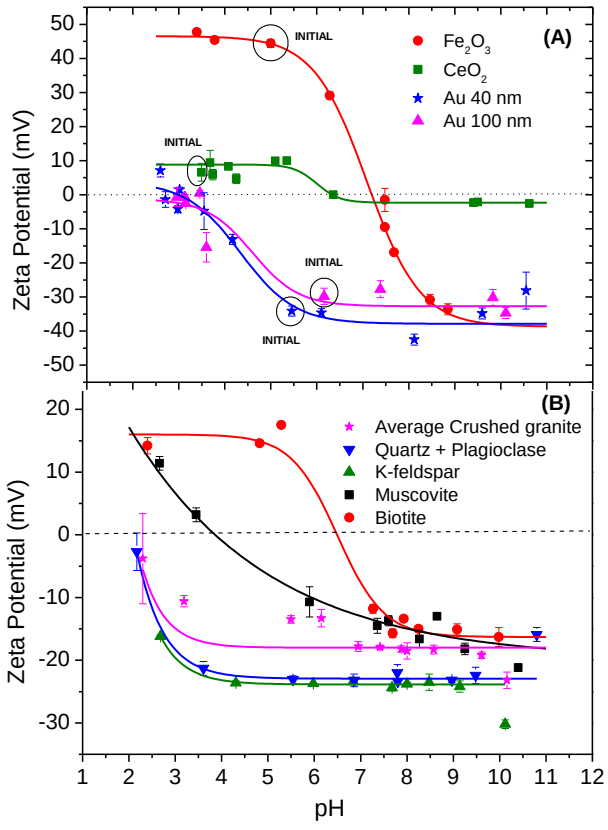

Figure 5: *(A) Zeta potential measured as a function of pH for Au colloids ($Size_{INI}$= 40 nm at pH6), CeO2 ($Size_{INI}$= 60 nm at pH 3) and Fe2O3 colloids ($Size_{INI}$= 100 nm at pH 5.28). (B) Zeta portential of main minerals composing granite as a function of pH.*

Table 2 presents a summary of colloid diffusion coefficients measured by RBS for the different colloids on different granite minerals, and at different experimental conditions. RBS results demonstrated that colloid access in-depth was equivalent in all cases, independently of the electrostatic interactions, so that it is mainly conditioned by colloid to pore sizes ratio and limited, since the colloid concentration inside rock was similar, independently of the colloid nature or the initial colloid concentration (from 50 to 1000 ppm).

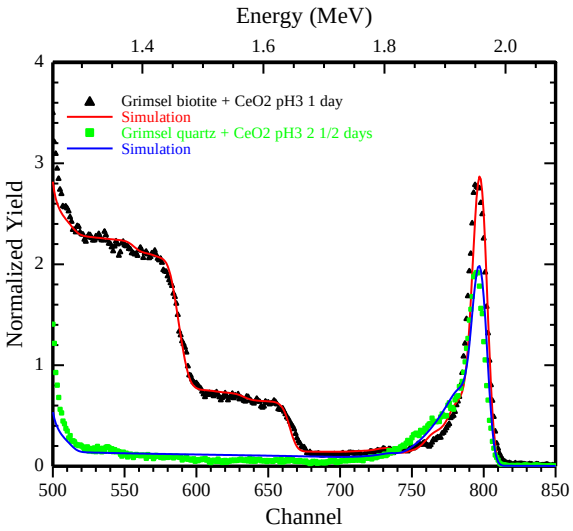

Figure 6: ***RBS spectra of granite minerals (biotite and quartz) after contact with CeO_2 colloids at pH 3. The spectra simulations are also included.***

Table 2: Colloid diffusion coefficients measured by RBS on different granite minerals at different experimental conditions.

Colloid	Size (nm)	pH	Pot. ζ	Mineral ζ (mV)	Da (m^2/s)
Au	20	6.2	-35 mV	Feldsp -25 mV	$(2.0 \cdot \pm 0.1) \cdot 10^{-18}$
Au	20	6.2	-35 mV	Biotite +15 mV	$(4.7 \cdot \pm 0.1) \cdot 10^{-18}$
Au	20	9.0	-30 mV	Felds -25 mV	$(1 \cdot \pm 0.1) \cdot 10^{-18}$
Au	20	9.0	-30 mV	Biotite -15 mV	$(3.4 \cdot \pm 0.1) \cdot 10^{-18}$
CeO_2	60	3.0	+8 mV	Quartz -15 mV	$(4.7 \cdot \pm 0.1) \cdot 10^{-18}$
	60	3.0	+8 mV	K-Feldsp -15 mV	$(4.3 \pm 0.1) \cdot 10^{-18}$
	60	3.0	+8 mV	Biotite +15 mV	$(1.9 \cdot \pm 0.1) \cdot 10^{-18}$
Fe_2O_3	60	4.5	+20 mV	Mica -12 mV	$(7.9 \cdot \pm 0.5) \cdot 10^{-18}$
Fe_2O_3	60	4.5	+20 mV	Quartz -15 mV	$(3.6 \cdot \pm 0.5) \cdot 10^{-18}$

As conclusion, colloid diffusion coefficients have been measured, for several sized and charged colloids, in different minerals in a natural granite. All diffusion coefficients measured

were in the range of $D_a = 10^{-18}$ m^2/s. No significant differences in D_a were measured amongst colloid of different charge but the main changes were attributed to size variations. Maximum surface distribution coefficients measured were $K_a = 3 \cdot 10^{-3}$ m.

2.2 Column migration studies (ÚJV Řež)

The transport of clay colloids, radionuclides (^{85}Sr, ^{137}Cs) and radiocolloids were studied in column arrangement. Columns were filled with crushed granitic rock from Melechov massif (depth 97.5-98.7 m, Czech Republic). The synthetic granitic water (SGW) and deionised water were used as liquid phase. The composition of SGW corresponds with composition of groundwater from Melechov massif. The process of preparing stable colloid suspension is described in Deliverable D3.2. The transport of tracers was described by breakthrough curves and by calculated transport parameters R (retardation coefficient) and K_d (distribution coefficient). The column experiments were used for studying of following issues:

- Influence of liquid phase composition on transport of radionuclides, clay colloids and radiocolloids;
- Sorption of radionuclides on clay colloids;
- Transport of clay colloids in granitic rock.

The presented conclusions are based on the experimental results. The transport of cationic radionuclides in the crushed granite simulating mainly transport in fissure infill or in some disturbed zone.

2.1.1 Can clay colloids be considered as radionuclide carriers?

For preparation of radiocolloid suspension see Deliverable D3.5. Preparing the colloid suspension for the column experiments about 80 % of radionuclides (^{85}Sr, ^{137}Cs) were sorbed on clay colloids. The influence of clay colloid particles on radionuclides transport was evident from comparison of breakthrough curve of radionuclide in the presence and absence of clay colloids (see Deliverable D3.5, D3.8). The migration of radionuclides through crushed granite in presence of clay colloids was faster, so the clay colloids played a role as a radionuclide carrier. The explanation is, that the clay colloids carried the radionuclides further into the column and then desorbed from the colloidal phase onto the granite surface. The difference between Sr and Cs was that minor part of Cs (2 %) was irreversibly sorbed on clay colloids under the hydrodynamic conditions prevailing and thus the cesium was measured in column outlet immediately from the beginning of experiment (see Fig. 7).

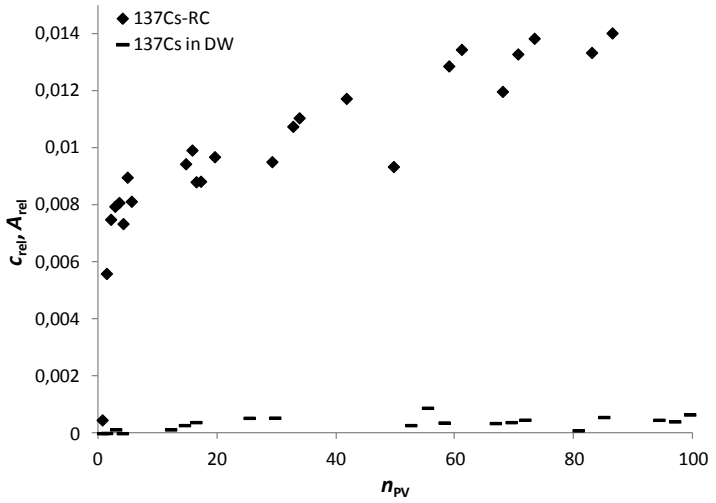

Figure 7: *The breakthrough curves of ^{137}Cs through granite in presence of clay colloids (-) and without (♦).*

2.1.2 Is there an upper bound for colloid-mediated transport?

The liquid phase properties (e.g. ionic strength, composition) are one of the most important parameters, influencing the radionuclides transport. For system simplification, all migration experiments with radionuclides, colloids and radiocolloid were performed in deionised water. However, radionuclide behaviour in deionised water and groundwater may differ from each other. For this reason we studied the transport of radionuclides also in synthetic granitic water (SGW). The results showed the completely different behaviour of ^{85}Sr, ^{137}Cs in deionised water and in SGW. Migration of radionuclides through granite in SGW was faster than migration in deionised water. Very probably the transport was influenced by the presence of other ions in SGW (see Fig. 8). The rapid transport in SGW was caused by the competition effect of the cations in SGW, which occupied sorption sites in granite structure and limited radionuclide sorption.

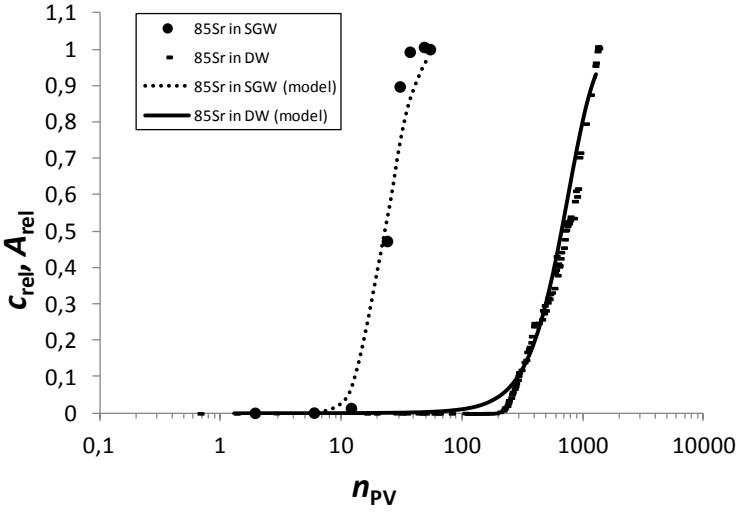

Figure 8: *The breakthrough curves of ^{85}Sr in SGW (•) and DW (-).*

2.2 Understanding the colloid and rock mineral interaction as a function of solution chemistry and rock surface heterogeneity (KIT)

Various factors contribute to the transport/retention of nanoparticles in the granitic environment including chemistry at the interface (pH, ionic strength), hydrodynamics, particle morphology and concentration etc. In general, bentonite colloids and most of the mineral constituents of the granite are negatively charged over wide span of pH range. Recent experimental results performed at Grimsel suggested significant loss of colloids even under glacial melt water conditions (pH=9.6). The recent studies performed at KIT-INE highlighted the importance of surface inhomogeneity to explain particle retention mechanisms, where minor topographic deviations can influence the particle deposition (Darbha et al., 2012b). The current aim finds the basis to understand the factors responsible for particle retention under these unfavorable electrostatic conditions.
The themes of this work are to predict the particle deposition as a function of 1) surface heterogeneity of substrate and effect of concentration of metal ion (Eu(III)) 2) Effect of fracture orientation on particle retention 3) Predicting the fundamental forces responsible for particle retention

2.2.1 Influence of surface roughness of granodiorite and Eu(III) concentration on colloid deposition efficiency

The granodiorite sample is from GTS, Grimsel, Switzerland. It is composed of quartz (27-28%), plagioclase (29-33%), K-feldspar (12-24%), biotite (7-11%) and clay minerals (0-1%) by volume. The minerals plagioclase, K-feldspar, and quartz minerals were purchased from Dr. F. Krantz GmbH, Bonn, Germany. Biotite mineral was purchased from WARD'S Natural Science, NY, U.S.A. Samples (granodiorite, quartz, plagioclase, K-feldspar and biotite) of approximately 1 x 1 x 0.4 cm^3 were exposed to polystyrene colloids of 1 µm size in an open-fluid cell (flow velocity 0.02 mL/min) for 60 min. The surface topography characterization (roughness parameters: *Rq, Rt, R10z, F*) and colloid quantification (Sherwood number, *Sh*) was done by VSI.
An increase in both roughness (*Rq*) and Eu(III) concentration increased colloid deposition efficiency on granodiorite. In the absence of Eu(III), an increase in *Rq* for surface sections from 450 to 1100 nm showed an increase in *Sh* by a factor of 24 (Darbha et al., 2012a). A large variation in deposition efficiency is predominantly influenced by roughness variations. Half-pores that exist on the rock in-between crystals (intergrannular porosity) have major impact on colloid retention. An increase in porosity results in enhancement of colloid sorption for [Eu(III)] $\leq 5x\ 10^{-7}$ M. Site-specifically, colloid deposition was predominantly along the pore-walls influenced by the sub-micron scaled protrusions. At higher Eu(III) concentrations ($\geq 5\ x\ 10^{-7}$ M), the sorption of colloids is independent of pore volume. This is due to the sorption of Eu(III) to smooth surface portions where $Sh_{smooth\text{-}portions}$ dominates $Sh_{\text{pore-volume}}$. The protrusions along half-pores diminish the overall DLVO interaction energy (due to lower contact area between colloids and substrate) between particles and surfaces rendering favorable for deposition. Moreover, the hydrodynamic shear forces acting on the mineral substrate are at maximum adjacent to colloids and reach a minimum along half-pores, i.e. the

rear stagnation point. This provides higher collision frequencies due to increased residence time and finally results in enhanced colloid retention. Our study showed that the colloid sorption is clearly favored at surface sections with high density of small asperities (density= 2.6 ± 0.55 μm^{-1}, asperity diameter= 0.6 ± 0.2 µm, height= 0.4 ± 0.1 µm) in contrast to surface sections with larger asperities and lower asperity density (density = 1.2 ± 0.6 μm^{-1}, d = 1.4 ± 0.4 µm, height = 0.6 ± 0.2 µm). Mineral-specific particle retention experiments were further carried on individual mineral surfaces. An enhancement of colloid deposition with change in [Eu] from 0 to 10^{-6} M was observed which can be ranked in the order K-feldspar K-feldspar(1.1)>quartz(5.8)>biotite(6.4)>plagioclase(7.4). The root-mean square roughness (*Rq*) of mineral is ranked as: K-feldspar (357 nm) >plagioclase (182 nm) >quartz(182 nm)>biotite(111 nm). Only a partial correlation between the roughness versus particle retention was observed. These results indicate that the increase in particle retention on complex granodiorite is not only from the electrostatic forces and heterogeneous Eu distribution on the mineral surface but also the roughness (half-pores) and the exposed edge-sites of silicate minerals where they are known to be positively charged at pH 5 are responsible. **Thus intergranular porosity of granite rock has an influential role to retain particles over intragranual porosity.**

2.2.2 Effect of fracture orientation on particle retention

To elucidate the particle retention as function of fracture orientation, particle transport experiments were performed by a highly controlled (well defined) fluid cell is designed at KIT-INE that provides feasibility to open the fracture after the flow experiments for detailed post mortem analysis. Also the effect of gravity (particles with varying diameter 25 & 1000 nm) on particle retention was studied. The current study includes 1) prediction of overall colloid deposition efficiency from real-time fluorescence experiments 2) post mortem analysis of the granodiorite samples: a) quantifying colloids on defined areas using fluorescence microscopy b) identifying the mineral distribution on these areas using SEM and Laser Scanning Microscopy (LSM) and obtaining surface roughness parameters (*Rq*) c) correlating the surface roughness parameters to the colloid deposition values to predict mineral-specific particle deposition.
The artificial fracture cell set-up and the experimental approach including the post-mortem strategy has been documented in detail in deliverable 3.7.

The results of the continuous flow experiments with an applied flow rate of 7 mL/h (and one time of 2 mL/h) for both particle sizes and both fracture orientations have been conducted. The calculated residence time of the particles in the fracture is around 7 min. Figure 9 shows the BTCs of the experiments conducted with a horizontal fracture orientation (left) and with a vertical fracture orientation (right). To compare the results with the conservative tracer, the BTC of Amino-G generated under the same transport conditions is additionally plotted in each diagram. Expectedly, results show earlier first arrivals and more pronounced tailings in the measured breakthrough curves for both colloid types compared to the conservative tracer. Due to the bigger particle size resulting in a higher dispersion (smaller diffusion coefficient) the shapes of the colloid breakthrough curves of 1000 nm particles differ more clearly from the solute tracer than for the 25 nm particles. Additionally the shape of the BTCs of the bigger particles is less smooth compared to the BTCs of the smaller ones.
The recoveries of the colloid experiments deviate in less than 3 % and all recoveries were

higher than 94 %. A slight decrease in recovery by decreasing the flow rate was observed for the experiment using 1000 nm particles with an applied flow rate of 2 mL/h in the horizontal fracture orientation. Slightly lower recoveries are observed for 25 nm particles compared to 1000 nm particles for equal transport conditions but no dependency of fracture orientation on particles retention can be detected. The 3D topographic data obtained from AFM supports the observed results where the *Rq* values of granite are nearly 4 times higher for 24 nm tip than compared to a 1000 nm colloid probe. This shows that 25 nm particle can intrude into porous structures along the granite surface where 1000 nm particles are subjected to steric hindrance (Stoll et al., 2015 (in preparation)). In addition to continuous flow, we have performed experiments stop-flow experiments. In all the experiments, no effect of fracture orientation on 25 nm was observed while even under minor residence times, 1000 nm are subjected to gravity effect.

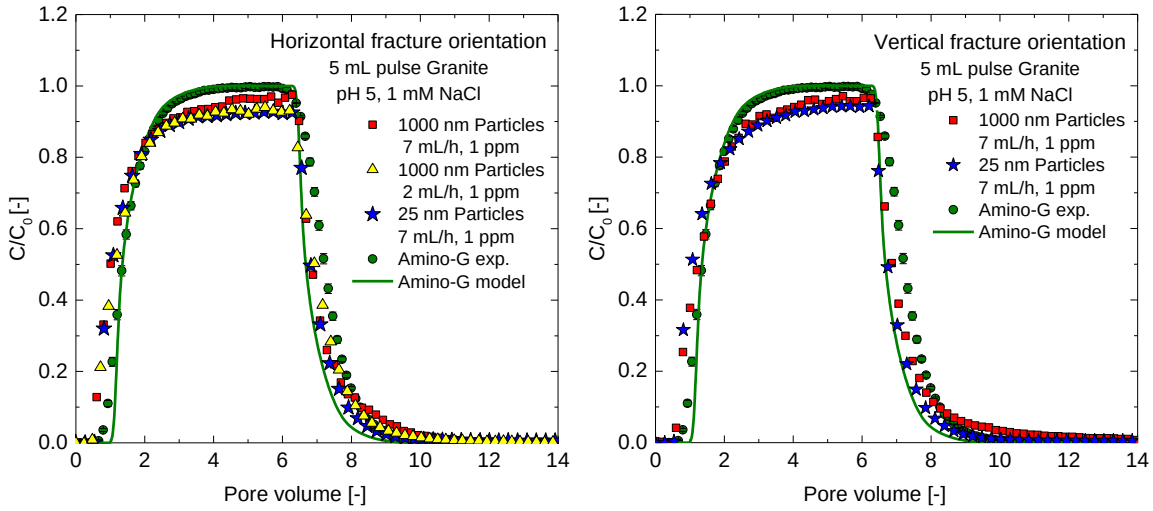

Figure 9: ***BTCs of continuous transport experiments using 25 nm and 1000 nm particles polystyrene particles at different orientation.***

The results of the post mortem analyses for these two colloid migration experiments are shown in Figure 5 (deliverable 3.7). This shows that irrespective of particle loading (even at high concentration that increases probability of bombardment with substrate), the particles tend to deposit only onto chemically and electrostatically favourable sites. The particle tends to avoid regions that increases charge repulsion barrier between them (unfavourable sites).
A positive correlation can be observed between colloid deposition efficiency and the surface roughness has been documented in deliverable 3.7 for *Rq* >10 µm. The trend dependency of *Rq* on *Sh* is higher at low colloid concentrations.
A prediction of the particle number on the whole reactive surface is possible by summarizing the counted particles for every ROI and making an extrapolation for the entire flow-wetted surface (deliverable 3.7).

2.2.3 Predicting the fundamental forces responsible for particle retention

The interaction forces between colloids (clay edge-site reactivity) and minerals surfaces were analyzed by AFM using colloid probe technique where a colloidal particle (Al_2O_3 or SiO_2) is attached at the end of AFM cantilever. The in-situ force measurements were possible using a home-designed fluid cell. Argon was purged into the stock solution and in the AFM chamber

continuously throughout the measurements.

As function of pH and Eu(III). An increase in pH increased the repulsive forces between both the applied particles (alumina and silica) and mineral surfaces. This is evident from the decrease in snap-in and adhesion forces measured at the interface and is in agreement with the reported magnitude of surface potentials (PZC of silica and alumina are 3.2 and 9.2 respectively). The range of repulsive forces between particles and surfaces are a measure of magnitude of charge at the interface. Though the measured snap-in forces are negligible (within the deflection error of the cantilever), at pH<6, the snap-in forces between silica and mineral surfaces are higher compared to alumina with the highest for K-feldspar (Figure 10). The measured PZC of K-feldspar is 5, hence higher the electrostatic forces between negatively charged silica colloid and positively charged K-feldspar. At pH > 6, the snap-in forces remained constant without any change. In the case of alumina, high snap in forces were observed for all minerals except for biotite at low pH. An increase in pH showed a gradual decrease in snap in forces due to increase in negative potential of the surfaces. In case of biotite the snap in forces were maximum at pH 6 indicating lowest interaction energy barrier (Darbha et al., 2015 (in preparation)).

The snap-in and adhesion forces between colloids (silica & alumina) versus granite surface were performed at varying pH (5 and 9). At pH 5, the ratio of snap-in forces between silica and alumina shows that, the silanol groups have more affinity towards mineral surfaces in the presence of [Eu] than aluminol groups. The reactivity of silinol groups towards mineral surfaces is high at $2x10^{-6}$ moles/L for K-feldspar and $4x10^{-6}$ moles/L in case of plagioclase. The predominant snap-in ratio (silica/alumina) towards K-feldspar (1750 times) indicates the preferential sites to play role in clay colloid deposition onto granite surface. The adhesion forces also depict increased silica reactivity towards minerals compared to alumina. As in the case of snap-in forces, though the ratios do not vary much, higher adhesion values are also observed for plagioclase. At pH 9, except for biotite, in general, the reactivity of silanol exceeded that of aluminol at all [Eu]. In the case of feldspars, an increase in pH showed an increase in reactivity of silanol to alumina by 2 to 4 times and the ratio is found independent of [Eu] indicating no influence of [Eu]. For biotite, it is a reverse effect, at pH 9, the reactivity of aluminol groups slightly exceeded to that of silanol groups.
In summary, this indicates that even under alkaline conditions, silica has more affinity towards major minerals of granite compared to alumina in the presence of [Eu].

As function of ionic strength. The force measurements were performed at pH = 5 and varying ionic strength (1 & 10 mM NaCl). As predicted by DLVO theory, a 10 fold increase in ionic strength showed an increase in adhesion forces between colloidal probe and surfaces. A similar trend of adhesion was observed between colloid and mineral surfaces independent of ionic strength. At 10^{-5} M Eu(III), from 1 to 10 mM NaCl the order of adhesion forces for Al_2O_3 are: plagioclase (5.76) > quartz (3.99) > biotite (2.41) > K-felspar (3.25). In the case of SiO_2 the order is: plagioclase (1.88) > K-feldspar & biotite (1.71) ≈ quartz (0.68). Overall, from the magnitude of pull-off forces, SiO_2-biotite adhesion forces dominate the remaining colloid-mineral interactions.

As function of surface roughness. Adhesion forces between four different Al_2O_3 colloid

probes of similar size (8 µm) against a smooth biotite (Root mean square roughness, *Rq* < 1-3 nm) as a function of pH was performed. Though similar trend of adhesion forces was observed with maximum at pH 6, a change in the magnitude of adhesion forces (1.2 to 2 time) was observed, which is attributed to the rough features (of ~10 nm range) along colloidal particle verified by SEM and AFM, which demonstrates the influence of roughness on particle adhesion forces.

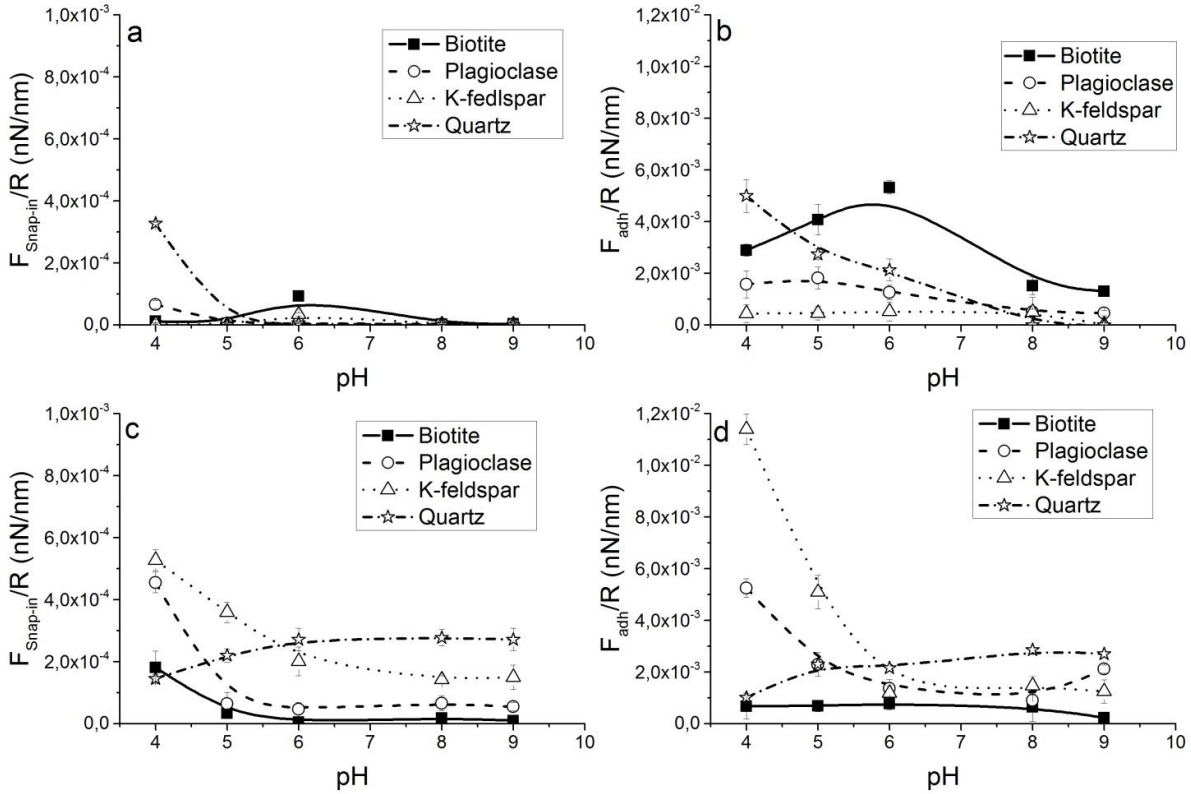

Figure 10: *(a & c) represent normalized snap-in forces between alumina and silica particle at varying pH in 1 mM NaCl. (b & d) represent normalized adhesion forces between alumina and silica particles at varying pH in 1 mM NaCl.*

Summary:

The current study reveals the importance of considering the surface heterogeneity of rock matrix into predictive colloid-associated-radionuclide transport in the geological environment. The highlights of the study are

- Roughness of granite plays a critical role at low metal ion concentrations (Eu <5x10^{-7} M addition to synthetic Grimsel groundwater). With an increase in the metal ion concentration chemistry at the interface dominates the particle retention over roughness effects
- An increase in *Rq* for surface sections from 450 to 1100 nm (cut granite disc) showed an increase in particle retention efficiency by a factor of 24. This signifies the estimation of *Rq* of natural granite fracture (which can be in the range of mm) and including this parameter for colloid deposition.
- Site-specifically, sheet silicates (majorly biotite) along the half-pores of the granite are

responsible for particle retention under glacial melt water conditions.

- A change in fracture orientation has no effect on smaller particles (25 nm) while the larger fraction (1000 nm) are subjected to gravity effect.
- The post-mortem analysis of the granite fracture reveals an increase in particle retention with roughness and along grain boundaries. Grain boundary effect is pronounced only at low colloid concentrations. Compared to intra-granular porosity, inter-granular porosity has less influence on particle retention.
- AFM-Colloid probe technique for estimating the reactivity of clay edge-site (aluminol versus silanol) shows that though for both colloids the repulsive forces dominate at pH > 6 in overall, SiO_2 has more affinity towards majority of the minerals over Al_2O_3.
- In the presence of Eu ($2x10^{-6}$M) at pH 5, the predominant snap-in ratio (silica/alumina) towards K-feldspar (1750 times) indicates the preferential sites to play role in clay colloid deposition onto granite surface. Under alkaline conditions (pH 9), in the presence of Eu, SiO_2 showed a 2-4 time higher reactivity compared to Al_2O_3.

2.5 Colloid migration experiments on crushed rocks and rock fracture columns (HU)

University of Helsinki studied colloid and radionuclide-colloid migration in the crushed rock, drill core and rock fracture columns. The crushed rock columns were made of intact, fine-grained granite and strongly and homogeneously altered tonalite. The crushed rock column diameter was 1.5 cm and length 15 cm or 30 cm. Drill core columns were constructed from Kuru gray granite cores which were placed inside a tube to form a flow channel (L = 68.5 cm, w = 4.4 cm) representing an artificial fracture formed by the 0.5 mm gap between the core and the tube. The rock fracture column from Olkiluoto tonalite drill core was artificially fractured along the natural fracture containing an altered zone and filling minerals witch where mainly chlorite. The fracture width in the column was about 3.5 cm, the column length 6.8 cm and the fracture aperture 100 μm. In the first experiments, colloid solution (3 g/L) was injected into the water flow as a short pulse. The experiments were performed in the low salinity Allard reference groundwater, in which the colloids are assumed to be stable and mobile. Colloid concentration was determined by analyzing the aluminum content of montmorillonite using ICP-MS. Details can be found in deliverable 3.5 and 3.8.

Migration of colloids was affected by the rock alteration, type and length of column, water flow rate and colloid size. The recovery of bentonite colloids in these experiments was low, the lowest recoveries were found in crushed rock columns (< 4 %). The highest recoveries were found in the drill core (30 %) and rock fracture columns (60 %). Slowing down the water flow rate, the recovery was decreased. However, the flowrates in these experiments were orders of magnitudes faster than the groundwater flow. The colloid recovery was determined also from the Np-237 migration experiments, where colloid solution was pumped continuously into the water flow. Colloid concentration was determined using a derived count rate obtained by PCS measurements and standard series. The recovery of colloids in the crushed rock column was 20 % and in the drill core column 30 - 40 %.

The effect of bentonite colloids on Sr-85, Eu-152 and Np-237 transport was studied in the

column experiments. The retardation factor was estimated from the breakthrough curves of the conservative tracer and the radionuclide when the same experimental conditions have been used. However, the retardation factor was an approximation, because in the course of column experiment equilibrium between sorbed and dissolved species may not have been attained. In the all columns particularly Eu-152 was strongly retarded but also Sr-85 was retarded without colloids. In the presence of bentonite colloids, the slow elution of Sr-85 was obtained. In the Olkiluoto rock fracture column, the retardation factor, R_f of 56 was estimated without the presence of colloids at water flow rate of 10 µl/min. In the presence of colloids, R_f of 7.1 was estimated. No breakthrough of Eu-152 activity was detected during two week experiment with or without the addition of bentonite colloids, whereas the initial Eu-152 association to the bentonite colloids has to be quantified. In these experiments, colloid solution (3 g/l) was injected into the water flow as a short pulse resulting in very low colloid concentration available. The effect of bentonite colloids on Np-237 transport was studied in Kuru Grey granite drill core and crushed rock columns. In the drill core column, no breakthrough of Np-237 was detected in the absence of colloids. In the presence of bentonite colloids, all injected Np-237 was eluted. In the crushed rock column, Np-237 was eluted slightly faster in the presence of colloids. These experiments performed in a small laboratory scale, showed that colloids had an effect on radionuclide transport. The main uncertainties remain still in the quantification of colloids under realistic repository conditions and how mobile colloids are. Thus, the assumption of the low contribution of colloids as radionuclide carriers cannot be validated properly based on these experiments.

3.0 Radionuclide sorption

3.1 Sorption isotherms and sorption reversibility (CIEMAT)

During the last years CIEMAT analysed radionuclide the sorption of different types of radionuclides (Eu, Pu, Sr, U, Cs, Cd, etc…) on bentonite was studied. In order to determine if the sorption is reversible or linear, detailed studies must be carried out.

Without being exhaustive of all the work carried out, Figure 5 shows an example of sorption isotherms for four different radionuclides, between those analyzed, in which the main sorption mechanism is indicated and if sorption is linear or not. Indeed, different sorption mechanisms will be dominant for each radionuclide also according to the specific chemical conditions.

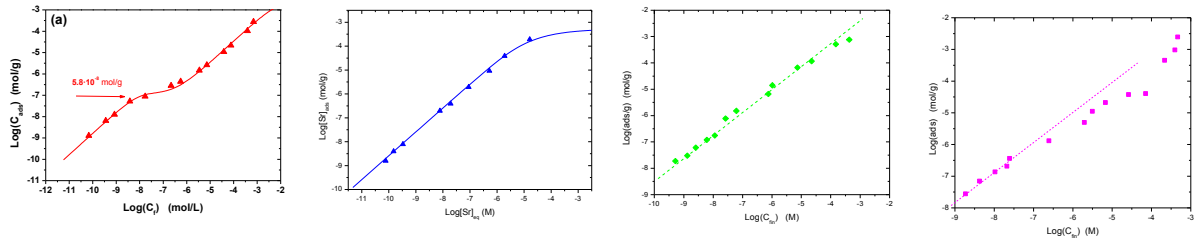

Cs: Cation exchange; Non linear.

Sr: Cation exchange and inner sphere surface complexation; Linear.

Eu (U): Inner sphere surface complexation and cation exchange; Linear.

Cd: Inner and outer sphere surface complexation and cation exchange; Linear.

Figure 11: ***Examples of sorption isotherms of different radionuclides on bentonite colloids. The sorption mechanisms are indicated as well as if their sorption is linear or not.***

The reversibility of the sorption process was tested with desorption tests. To evaluate the extent of sorption reversibility, the kinetics of the sorption and desorption processes was also analyzed. Desorption can be promoted by chemistry changes (Missana et al., 2004) or by the presence of a third phase (Bouby et al., 2011; Bryan et al, 2012).

In most of the cases investigated, the sorption K_d were similar to desorption ones, basically indicating sorption reversibility. Sometimes, small sorption/desorption hysteresis has been observed.

Only in the case of Cs, an irreversible retention mechanism was clearly observed: i.e. the incorporation in the frayed edge sites of the illite/smectite mixed layer (Missana et al., 2004). Cs was also the unique case in which sorption was clearly nonlinear.

Most recently, in the BELBAR project desorption processes promoted by increase of ionic strength was analysed in the case of cadmium onto FEBEX bentonite colloids. For sorption/desorption experiments, bentonite was conditioned in Na- homoionic with $NaClO_4$ as described in (Missana et al., 2008a).

Studies were carried out with ^{109}Cd, to a final Cd concentration of $1 \cdot 10^{-5}$ M, adding $CdCl_2$ (Merck).The Cd stability constants and speciation was verified (Powell et al., 2011; Zirino and Yamamoto, 1972) and the selected Cd database is reported in (Alonso et al., 2016). Considering the presence of Cl^- and $HCO3^-$ as organic ligands, Cd^{2+} is the dominant aqueous species up to pH 8 with and around 5% presence of $CdCl^-$. The hydrolysed species $Cd(OH)^+$ starts playing a relevant role for pH higher than 8.

The kinetics of the sorption process was first analysed at three different pH (4, 7 and 10). At pH 4 and 7 the K_D measured after 1 day of contact remained constant up to 30 days, but at pH 10 sorption slightly increases over time, as can be seen in Figure 12.

Once selected kinetic contact time elapsed, $NaClO_4$ was added to the four remaining samples of each pH set, to increase ionic strength from 10^{-2} M to 10^{-1} M and maintained in continuous stirring during selected desorption times (1, 7, 15 and 30 days). The cadmium concentration (M) measured in the liquid phase (M) as a function of time after increasing ionic strength to 10^{-1} M is presented in Figure 12, for the three studied pH: 4, 7 and 10 (Mayordomo et al, 2014). In the Figure, the time scale of desorption experiments is presented considering the initial pre-equilibrium time at the lower ionic strength 10^{-2} M (1, 15 or 30 days).

At pH 4 and 7, Cd concentration in the liquid phase increases after 1 day, and values are constant upon time, indicating Cd is reversible. At those pHs, Cd sorption on bentonite is expected to occur by cation exchange (Missana et al., 2015b) so that a decrease in sorption (concentration increase in the liquid phase) by increasing ionic strength is expected. The obtain values decreasing ionic strength at fully comparable to those measured at 10^{-1} M (Missana et al., 2015). Considering that absence of kinetics is observed in any case, Cd sorption on bentonite for pH 4 and 7 can be considered reversible. Indeed, it is generally assumed that cation exchange process is fast and reversible (Stumm, 1992), showing the same sorption and desorption rates. Cadmium sorption reversibility from other clays was observed (Comans, 1987). To calculate Cd dissociation constants, shorter experiments should be carried out because at pH 4 and 7, both sorption and desorption are complete after one day.

However, the Cd desorption at pH 10 presents much complex behaviour than in the above mentioned cases (Figure 12). At pH 10, Cd sorption is expected to take place by surface complexation (Missana et al., 2015b) and Cd sorption increased over time. Kinetics of desorption experiments showed a dependence on initial pre-equilibrium time, what suggests that Cd is not fully reversible, under these conditions surface complexation dominates.

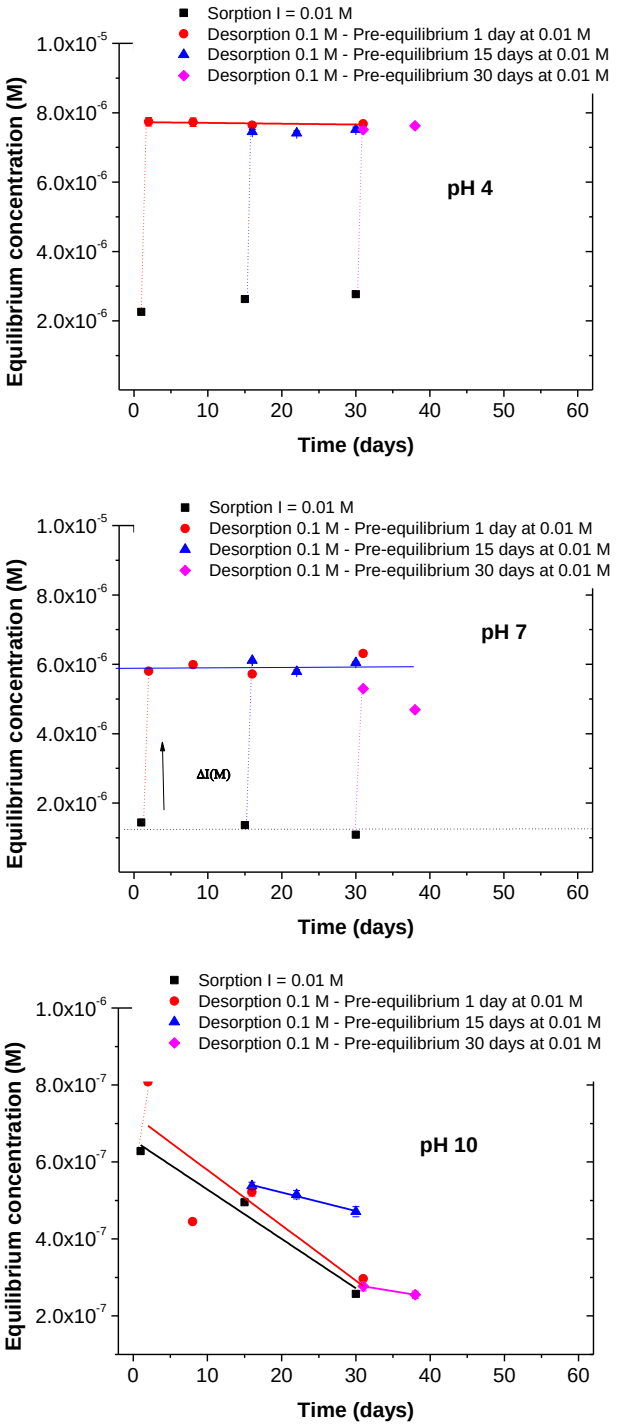

Figure 12: ***Cadmium concentration (M) measured in the liquid phase (M) as a function of time after increasing ionic strength to 10^{-1} M to promote desorption at three different pH: 4, 7 and 10. The time scale of desorption experiments is presented considering the initial pre-equilibrium time at lower ionic strength 10^{-2} M (1, 15 or 30 days).***

To evaluate the sorption reversibility under dynamic conditions, transport experiments were designed to favor high recovery of the particles i.e. using high enough water flow and checking the recovery of radionuclide in parallel to that of colloids.

Table 3 shows a comparison of tests performed with different radionuclides under Grimsel ground water conditions. In all the cases, sorption onto the bentonite particle was medium-high, but the fraction of radionuclide that was actually transported without retardation, along with the colloids, was much lower than the initially adsorbed on them. These results indicate that sorption on colloids is at least partially reversible (Missana et al., 2008b). Desorption from the colloids is a very important factor limiting the role of colloids in radionuclide transport.

Table 3: ***Comparison of transport tests performed with different radionuclides.***

Element	Initially adsorbed on colloids	Transported "unretarded" with BC
Sr	> 80%	< 2 %
Eu	> 80%	< 7 %
U	~ 30 %	<1 %
Cs	> 80%	0.15 %

3.2 Eu(III)/Am(III), Th(IV) and U(VI) bentonite colloids dissociation (UNIMANCH)

Deep geological disposal is a method of managing high level, long-lived nuclear waste. It is a concept that many countries are exploring for the possibility of managing nuclear waste generated from power production. For deep geological disposal to be viable then areas where problems may surface have to be explored. Bentonite clay has been proposed as the material to be used for the backfill of the repositories. Its swelling properties ensure that it will expand to plug the bore holes that will be made for the waste, its impermeable nature restricts contact between groundwater and the waste package and its stability on a geological timescale all make it desirable as a backfill material. This project looks at the role that colloids formed from the bentonite clay could have in facilitating radionuclide transport away from a nuclear waste repository. Several radionuclides (Eu(III), U(VI), Th(IV) and Am(III)) have been considered. Ternary systems of ^{152}Eu(III), bulk bentonite and EDTA ([Eu] = 7.9 x 10^{-10} M; pH = 6.0–7.0) have been studied. Without EDTA, there was slow uptake in a two-stage process, with initial rapid sorption of Eu(III) (96%), followed by slower uptake of a smaller fraction (3.0 % over a period of 1 month). The reversibility of Eu(III) binding was tested by allowing Eu(III) to sorb to bentonite for 1-322 days. EDTA was added to the pre-equilibrated Eu bentonite systems at 0.01M. A dissociation rate constant of approximately 4.3 x 10^{-8} s^{-1} (values in the range 2.2 x 10^{-8} - 1.0 x 10^{-7} s^{-1}) for pre-equilibration times ≥ 7 days was measured. Eventually, the amount of Eu(III) remaining bound to the bentonite was within error of that when EDTA was also present prior to contact (4.5 % ± 0.6). Eu interactions with colloidal bentonite were studied, and the dissociation rate constant measured by a resin competition method. A dissociation rate of 8.8 x 10^{-7} and a range of 7.7 x 10^{-7} – 9.5x 10^{-7} s^{-1} were measured. For both bulk and colloidal bentonite slow dissociation was observed for Eu(III), but there was no evidence for 'irreversible' binding. The interactions of ^{232}U(VI) with bentonite colloids ([U] = 5.43 x 10^{-10} M; pH = 8.8 ± 0.2) have been studied using a resin ion

exchange competition technique. The reversibility of the interaction was studied by allowing U(VI) to sorb to bentonite colloids for periods from 1-35 days. A fraction of the U(VI) was removed from the solution instantaneously (28-50 %), and after 3 days, the amount of U(VI) remaining on the bentonite colloids was 17- 25%. With time, the amount of U(VI) retained by the bentonite colloid is reduced further, with a first order dissociation rate constant of 5.6 x 10^{-7} s^{-1}. Whilst the dissociating fraction was small (24% (+34; -12 %)), complete dissociation was not observed. Although slow dissociation was observed for U(VI), there was no convincing evidence for 'irreversible binding' of the radionuclide by the colloid. The interactions of ^{228}Th(IV) ([Th] = 3.79 x 10^{-12} M; pH = 8.8 ± 0.2) and ^{241}Am(III) ([Am] = 3.27 x 10^{-9} M; pH = 8.8 ± 0.2), with bentonite colloids have been studied using an ion exchange competition technique. Th(IV) was not fully associated with the bentonite colloids, and filtration showed that the uptake after 1 week was 78.3% (± 2.7%). Am(III) was weakly associated to the bentonite colloids, the uptake after 1 week was 20.1 % (± 5.2 %). Cellulose phosphate was added to the radionuclide/bentonite colloid systems (1 g for Th(IV), 0.2 g for Am(III)), an amount that was sufficient to retain the radionuclide when no bentonite colloids are present. A fraction of the Th(IV) is initially removed by the Cellphos (75-93 %), and after 7 days the amount of Th(IV) remaining on the colloids is 1- 3 %. Over the time of the experiment, the amount of Th(IV) retained by the bentonite colloid appears to remain level and the amount bound to the bentonite colloid at the end of the experiment is 2.1 % ± 0.88 % which is within experimental error of the steady state equilibrium of the system. A fraction (48-94 %) of the Am(III) is also initially removed by the Cellphos, after 7 days the 9 amount of Am(III) remaining on the colloids is 1.2 – 9.3 %. However, after 35 days of contact time with the cellulose phosphate it appears that Am(III) is released back into the system, preventing dissociation rates from being calculated in this case. Studies of the association of Eu(III) to the clay colloids and its subsequent dissociation in this thesis follow similar trends to those described elsewhere in the literature (Missana et al. (2008a), Bouby et al. (2011)). The Eu/bentonite colloid dissociation rate calculated here (8.8 x 10^{-7} s^{-1} (± 9.1 x 10^{-7} s^{-1})) is within error of the dissociation rates for trivalent ions estimated by SKB (2010) (Am(III) 5.6 x 10^{-7} s^{-1} Cm(III) 1.7 x 10^{-6} s^{-1}). The U(VI) studies in this thesis show a dissociation rate of 5.6 x 10^{-7} s^{-1} (± 4.2 × 10^{-7}) which is within error of the U(VI) dissociation rate estimated by SKB (2010) (8.3 x 10^{-7} s^{-1}). Reliable dissociation rates could not be obtained from the Am(III) and the Th(IV) studies in this thesis, other studies (e.g. Bouby et al. (2011)) showed signs of irreversible binding of Th(IV) to bentonite colloids, however, no irreversible binding was observed in this thesis. Am(III) did not appear to be a close analogue of Eu(III) in these systems, which is very surprising. All of the isotopes studied in this thesis showed no evidence of irreversible binding to bentonite or bentonite colloids. As such, the role that bentonite colloids will have in the facilitated transport of radioisotopes away from a repository is likely to have only a limited impact, at most, on the environmental safety case.

3.3 Sr and Cs reversibility experiments (ÚJV Řež)

The dynamic experiments showed the different behaviour of clay colloids in deionised water and clay colloids originating from radio-colloid suspension (Sr and Cs) through crushed granite. The clay colloid migration in deionised water in absence of other species was fast and comparable with the conservative tracer tritium. However, the transport of clay colloids in

presence of radionuclides was slower (see Fig. 13). This delay was probably caused by reactions in the system granite-colloids-radionuclide.

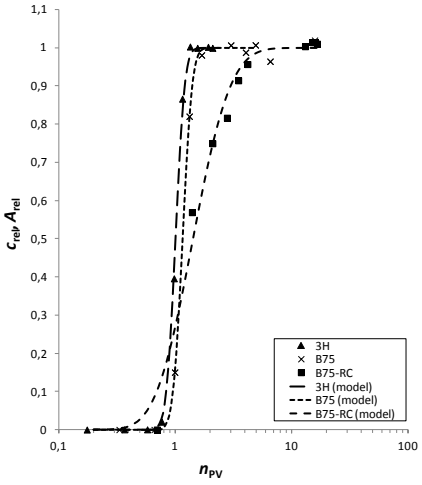

Figure 13: ***The breakthrough curves of tritium (▲), bentonite colloids (×) and bentonite colloids of radiocolloid suspension (■).***

Reversibility or irreversibility of radionuclides (Sr and Cs) sorption on clay colloids was studied by dynamic column experiments (see Deliverable D3.5, D3.8). The fully reversible sorption on clay colloids was observed in case of strontium (see Fig. 14A). Immediately after entering into the column, the strontium was completely desorbed from clay colloids and was retained in granitic rock. The strontium sorption was strong (K_D was 56.2 ml/g). In case of cesium, major part (98 %) was sorbed on the granite and minor part (about 2 %) left the column together with clay colloids. The resulting K_D was 81.6 ml/g. The different behaviour of cesium and strontium transport is assumed to be the result of different radionuclide sorption mechanisms on clay colloids. There are two important sorption sites for cations on the bentonite surface. Firstly, there are the planar sites in bentonite interlayers. These sites are available for most cations and sorption is weak and reversible. The strontium and cesium were sorbed on these easily accessible sites. The second type of sorption sites are frayed edge sites (FES). Sorption on FES is very limited, the FESs are accessible for smaller, non-hydrated cations and sorption is very strong and irreversible. About 2 % of cesium was sorbed on the FES in bentonite structure and left the experimental column without retardation (see Fig. 14B).

The linearity of Cs and Sr sorption on bentonite is widely known. For Rokle bentonites, the Cs linear sorption is generally observed in the concentration range 10^{-6} – 10^{-2} mol/L (planar sites in bentonite interlayers). The non-linear sorption occurs for lower concentration < 10^{-7} mol/L (frayed edge sites); see Fig. 11 (CIEMAT data). For Sr the linear sorption is generally observed in the whole concentration range up to 10^{-1} mol/l (10^{-4} mol/L in Fig.11 of CIEMAT data). The upper limit depends on cation exchange capacity of bentonite.

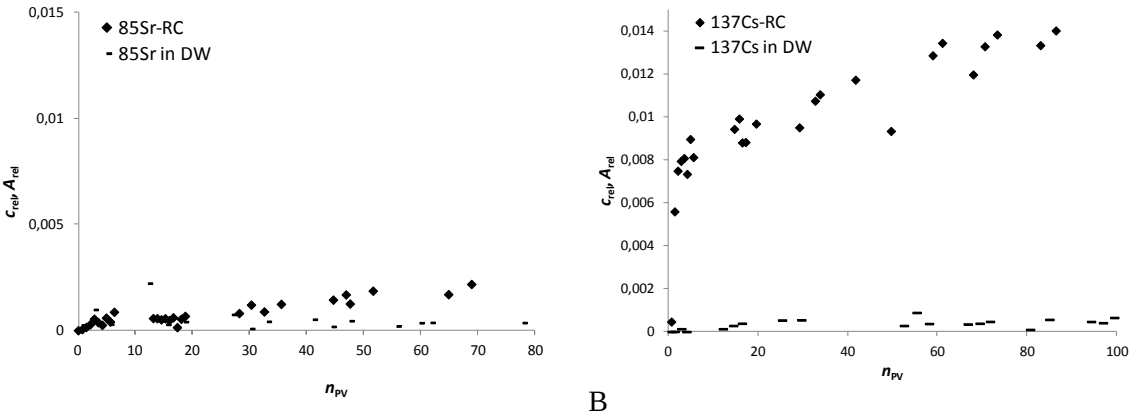

Figure 14: ***The differences between radionuclides behaviour in presence and absence of clay colloids.***

In summary, the experimental results showed that in presence of clay colloids the transport of radionuclides is faster. According to sorption reversibility or irreversibility the migration of radionuclides can be limited (reversible sorption on clay colloids) or supported (irreversible sorption on clay colloids). For both radionuclides (Sr and Cs) the affinity towards the granitic rock was higher than towards clay colloids (reversible sorption). In case of Cs, minor part (2 %) was irreversible sorbed on so called "freyed edge sites" of clay colloids (irreversible sorption). Colloid-mediated transport strongly depends on the composition of liquid phase, because the colloid stability is influenced by ionic strength of liquid phase (coagulation) and competition effect on sorption sites between ions and radionuclides in liquid phase can speed-up the transport. The clay colloids itself passed through crushed granite without retardation and behave as conservative tracer.

3.4 Colloid size effect on Th(IV), U(VI), Np(V), Tc(VII) and Pu(IV) sorption and reversibility (KIT-INE)

RN adsorption (Th(IV), U(VI), Np(V), Tc(VII) and Pu(IV)) onto size fractionated montmorillonite colloids (suspensions S0, S1, S2, S3, S3.5, S3.5,UC) was studied in a synthetic, carbonated groundwater (ionic strength (IS): 1.6×10^{-3} M, pH 8.4). Fractionation was done by simple settling procedures and sequential centrifugation. We combined batch adsorption experiments and geochemical modelling for the sorption studies.
U(VI), Np(V) and Tc(VII) did not adsorb to any montmorillonite size fractions in the synthetic groundwater. They remain as mobile aqueous species.
Adsorption of Th(IV) and Pu(IV) is strong but, within experimental uncertainties, not significantly affected by the fractionation process.
Montmorillonite clay colloids obtained by fractionation of the raw clay material but in the presence of organic matter during the initial separation step (S3.5, UC, FA) present a significantly reduced uptake of Th and Pu.
Based on the results, implementation of an "average log K_D" (i.e. average distribution coefficients) for all colloidal sizes in reactive transport modelling codes would be acceptable.

Conclusions: The size of the colloids does not seem to play a role on the RNs sorption

retention process. Small clay colloids are miniatures of bigger ones and show no unexpected behaviour.
More details can be found in

- Norrfors et al., Applied Clay Science, 114, 2015, 179-189
- Norrfors et al, 2016, Applied Clay Science, doi:10.1016/j.clay.2016.01.017.

Reversibility study (preliminary conclusions: data under treatment!)

The reversibility or evolution of radionuclide (Th, U, Np, Tc and Pu) sorption onto 7 size-fractionated montmorillonite colloids after 1) decreasing pH, or 2) increasing ionic strength or 3) adding crushed bedrock material (CBM) or 4) fulvic acids (FA) as competing ligands was examined. This was investigated for various contact times (3 days, 2 weeks, 1 month, 6 months) before the desorption/reversibility test starts

1. pH decrease: 1 week at pH 7.5, 1 year at 2.7

- Np: unaffected, whatever the initial contact time, remains "free" in suspension. The term "free" is used for "aqueous species".
- Tc: remains free after 1 week at pH 7.5; after 1 year at pH 2.7 the free Tc fraction represents > 80%, the rest is found under particulates (eigen-colloids and/or Tc-associated to sedimented clay colloids).
- U: after 1 week at pH 7.5, U is sorbed onto the different montmorillonite size fractions as the competition with carbonates is lower at that pH except in the suspension containing originally FA which compete with the clay colloids for the U sorption. After 1 year at pH 2.7, the U is found 100 % free in suspensions. The sorption is reversible at that rather low pH.
- Th: is initially sorbed (> 95 %) to all clay colloidal fractions, it does not change after decreasing the pH during 1 week at 7.5. If FA are present initially, less Th is initially clay colloid sorbed (~ 15 % less) and the decrease to pH 7.5 increases the amount of Th –FA-complexes significantly (~ 10 % more). This pH favours thus the complexation by FA and shows a partial Th sorption reversibility. After 1 year at pH 2.7, whatever the first sorption contact times, 80 ±5 % of the Th are desorbed from the clay colloids. The remaining clay sorbed fraction should be more clearly characterized. The Th sorption is partly reversible at rather low pH.
- Pu: whatever the contact times 85 up to 100 % Pu are sorbed to the clay colloidal fractions. In presence of FA it reduces down to ~ 70%. After one week at pH 7.5, the results are the same in the clay suspensions without FA, but in the one with FA, 40-60 % of the Pu only remains clay colloids associated. At that pH, the FA is a strong competitor of the clay colloids. After 1 year at pH 2.7 and in absence of FA, surprinsingly, only 10 to 15 % of Pu is free, the rest is found under particulates state. It is presently not possible to state precisely but it might corresponds to the sorption of Pu-eigen-colloids onto sedimented clay colloids (instable at that pH). This is still observed in presence of FA, even if in that case, to a less extend as 40-50 % Pu is found free or FA-complexed (as it cannot be distinguished). The Pu sorption is thus not reversible at that rather low pH.

2. Ionic strength increase: 0.5 M IS with $CaCl_2$, pH 7.4

At that IS, the clay colloids are instable and sediment.

- Np and Tc: are unaffected and remain free in suspension
- U: remains in suspensions. As this contradicts the results found by a decrease in pH to 7.5, it indicates the higher strength of the Ca-U(VI)-CO3 complexes compared to the U(VI)-colloid-bound species.
- Th and Pu: previously sorbed remain associated with the clay colloids which sediment.

Conclusions: at that high ionic strength and water conditions, the Np, Tc and U remain free in suspensions while the Th and Pu sorbed remain associated with the colloids and sediment.

3. Addition of crushed bedrock material (CBM): solid:liquid ratio is 1:4

The clay colloids do not interact with the CBM.

- Np: is transferred to the particulate phase whatever the colloidal size fraction investigated. This is kinetically controlled: 50 ± 10 % of Np are transformed after 1 week and ~100 % after 1 year. This might be attributed to the slow reduction of Np(V) to Np(IV) accompanied by the formation of Np(IV)-eigen colloids. This can be explained by the presence of iron into the granidiorite.
- Tc: behave like Np
- U: after 1 week, ~ 60 to 80 % are sorbed onto the CBM. This percentage is reduced after 1 year which might be due to the competition with the carbonates or the release of natural U from the CBM.
- Th: is initially mainly sorbed to the clay colloids. After 1 week of desorption contact time with the CBM, the results are the same. But after 1 year, drastic changes are observed where the contact time prior to the addition of the CBM and the clay colloidal size fractions play a role. A longer sorption contact time reduces the desorption in favour of the CBM and the smaller clay colloid sized fractions (mean size < 250 nm) keeps better sorbed the Th.
- Pu: behaves like Th.

Conclusions: In presence of CBM, under that water conditions, Np, Tc and U are sorbed and immobilized. Th and Pu sorption to clay colloids is partly reversible in presence of CBM, it is lower for increasing sorption contact time before desorption, and significantly reduced for the smallest sized clay colloidal fraction.

4. Addition of FA (5 mg·L^{-1}) with a delay, i.e. after different contact time

- Tc, Np and U: are unaffected and found as aqueous species in suspension. Note that it was presently not possible to distinguish the FA-complexes from any other aqueous species.
- Th: no strong desorption (not more than 10 % after 1 year), whatever the clay colloidal size fractions. The partial Th reversibility might be slightly more pronounced for the smallest clay colloidal size fraction.
- Pu: The shorter was the sorption contact time before the addition of FA, the higher is the desorption/complexation by the FA which can reach up to 20%. In addition, a higher desorption/complexation is observed for the smallest clay colloid size fraction (<250 nm). Nevertheless, even after 1 year desorption time, the

reversibility is not complete.

More details can be found soon in

- Norrfors et al, 2016, Applied Clay Science (in preparation).

Overall conclusions from this study: The full reversibility is not guaranteed based on the current status and reversibility kinetics are strongly depending on the geochemical parameters (pH, IS, competing material).

4.5 Sorption of Np(V) onto bentonite samples from Khakassia deposit, Russia (MSU)

In this work sorption behavior of Np(V) onto Khakassia clay (Russia) was studied. Various techniques, e.g. XRD, XRF, BET absorption, Mössbauer etc. were used to characterize clay. Bentonite from Khakassia deposit contains montmorillonite in the sodium form (66%) and rather high amount of kaolinite (5.5%) and non-clay impurities like quartz, feldspar, and calcite (3%).
XRF shows that Khakassia sample contain 3 % of iron. Speciation of iron was found combining results from Mössbauer spectroscopy. Sample from Khakassia deposit contain Fe(II) and Fe(III) species. Half of the iron present in intrinsic iron phase (most likely goethite). Other part of iron is structural iron in bentonite.
Np(V) sorption on different samples depending on pH values, time and ionic strength was established. $NaClO_4$ was used as electrolyte. The initial concentration of neptunium was $4 \cdot 10^{-14}$ M. Experiments were carried out under ambient conditions. It was found that steady-state equilibrium in all systems is reached in 1 day of equilibration. Figure 15 shows kinetics of Np(V) sorption onto studied clay at different ionic strength. It was found that during 1 hour sorption increases significantly. After this period of time sorption kinetics is much slower.

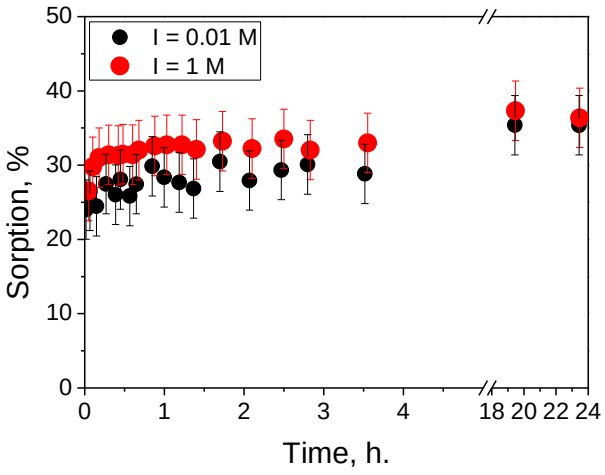

Figure 15: ***Kinetics of Np(V) sorption onto Khakassia clay at pH 8.3***

pH- dependences of Np(V) sorption onto studied clays at 0.01M and 1 M ionic strength are shown on figure 16. At pH higher than 6 sorption edges for different ionic strengths are

similar. It was found that ionic strength does not influence on Np(V) sorption onto Khakassia clay in this pH region. From that we proposed that surface complexation is the dominant mechanism of neptunium sorption. Due to low content of other minerals with high sorption ability (e.g. iron minerals, titanium oxides etc.) the main component affecting on Np sorption is montmorillonite.

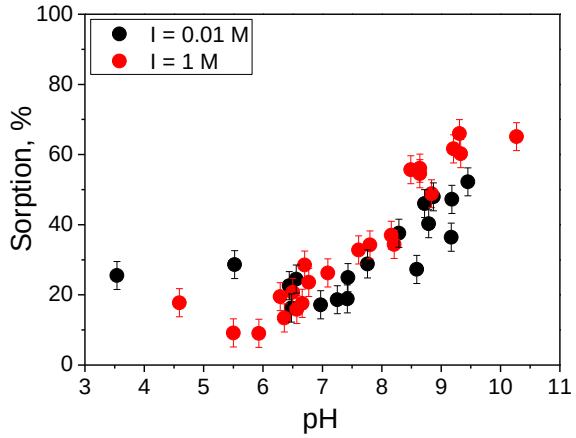

Figure 16: ***pH-dependence of Np(V) sorption onto Khakassia clay***

At lower pH sorption in 0.01 M $NaClO_4$ is higher that can be explain by ion exchange mechanism of interaction. The same conclusion was given by M. Zavarin et al. (2012) who studied Np sorption onto pure montmorillonite. Reduction of Np(V) was not observed during its sorption onto Khakassia clay.

These results are in a contradiction with previous results on Np sorption onto Khakassia bentonite (Sabonina et al., 2006). Previously it was also shown that neptunium sorption isn't affected by ionic strength, but the fraction of sorbed Np was higher than 50% already at pH 2. These differences can be explained by different redox conditions of experiment and solid to liquid ratio. In the present study the Eh values of suspensions were controlled by atmospheric oxygen, whilst the experiments of Sabonina et al., (2006) were carried out in glove box with inert atmosphere (N_2). It was shown that under unoxidized conditions neptunium reduced to Np(IV) can explain its high sorption. The solid to liquid ratio in Sabonina et al., (2006) was at least 10 times higher (from 6 to 100 g/L) than in the present study (0.5 g/L), that could also increase the sorption of Np.

The obtained results along with the results on plutonium sorption onto hematite colloids (Romanchuk et al., 2011) show that redox conditions and depending on them oxidation state have dramatic effect on the sorption of radionuclides and the kinetic of this process. The initial concentration of radionuclides in the range of femto- to nano- molar concentration does not have strong effect on the sorption kinetic and the distribution coefficient at equilibrium state.

4.6 Sr, Eu and Np reversibility studies (HU)

In the column experiments conducted at HU, no matrix diffusion was seen in the breakthrough curves owing to the high flow rates but also very low porosity of granitic rock.

University of Helsinki studied Sr-85, Eu-152 and Np-237 sorption bentonite colloids and suspension. The materials used were MX-80 Volclay bentonite (76 % montmorillonite), purified Na-Montmorillonite and Nanocor PGN Montmorillonite (98 %). Allard, low salinity granitic (I = 4.2 10^{-3} M) and diluted OLSO (I = 0.517 M) reference groundwater as well as electrolytes NaCl (I = 1 M – $1x10^{-7}$ M) and $CaCl_2$ (I = 3 M – $3x10^{-7}$ M) were used as solutions. OLSO simulates the current saline groundwater in Olkiluoto in oxic conditions.
Sr-85 and Eu-152 sorption on bentonite colloids was investigated as a function of ionic strength and pH (3 to 11). The sorption parameters as a function of pH were determined by conducting batch experiments in a clove box under CO_2 free conditions. The solid liquid–ratio was studied to obtain an optimum mineral concentration needed to conduct batch experiments, in which the amount of mineral or colloid is not the limiting the radionuclide sorption. The kinetic experiments were conducted to optimize the equilibration time for the batch experiments. The Zeta potential of the system was determined as a function of pH with and without a studied radionuclide in order to provide information about the adsorption mechanisms. Desorption experiments were done to investigate the reversibility of europium and neptunium sorption reaction on colloids and montmorillonite.

Strontium and europium adsorption onto the bentonite colloids and montmorillonite was highly pH dependent, adsorption increasing with increasing pH. Zeta potential of montmorillonite or colloid dispersion determined as a function of pH was negative from the beginning and decreased with increasing pH due to deprotonation and that the mineral surfaces were negatively charged across the pH range. Zeta potential was less negative with europium suggesting europium adsorption mechanism appeared not to be purely electrostatic but also via inner-sphere complex due to the aluminol sites present on clay minerals. In the case of strontium and cesium, no change in the Zeta potential curve was found meaning the sorption is based on electrostatic ion-ion interactions.

Np(V)-237 sorption on sodium montmorillonite and bentonite colloid dispersion made from MX-80 Volclay bentonite powder was studied under simplified but environmentally relevant conditions. Aluminium oxide (α-Al_2O_3), corundum was used as a reference mineral in order to study the aluminol surface sites present on clay minerals, which are regarded as the main adsorption sites for radionuclide attachment. Batch sorption experiments were done as a function of pH and neptunium concentration. The solid liquid–ratio was studied to obtain an optimum mineral concentration needed to conduct batch experiments, in which the amount of montmorillonite is not the limiting factor for the neptunium sorption. The kinetic experiments were conducted to optimize the equilibration time for the batch experiments. All sorption and desorption experiments were conducted in a N_2-glove box to exclude the formation of soluble Np- carbonato complexes that influence the uptake and speciation of Np on the solid surfaces.

Batch adsorption experiments showed an increased uptake of neptunium(V) on both mineral surfaces at pH-values above 7. Below this pH value, no adsorption of neptunium(V) on corundum was observed, while a constant sorption percentage of approximately 10 %, corresponding to ion exchanged neptunium(V) on negatively charged planar sites, was obtained for montmorillonite. Neptunium(V) uptake by ion exchange was confirmed in desorption studies. Desorption of neptunium(V) was observed over 250 h and found to reach

a plateau at a sorption percentage of approximately 15 %, where no further detachment of the actinide from the mineral surface could be detected. In desorption experiments at constant pH (pH 8, 9 and 10) almost complete removal of neptunium(V) from the montmorillonite surface was obtained at pH 8, whereas at pH 10 the amount of desorbed neptunium(V) was clearly decreased, indicating a change from outer-sphere to inner-sphere complexation in this pH range. Because experimental parameters such as the ionic strength or pH were not changed during the course of the desorption experiment, the neptunium(V) detachment from the surface could only be explained by fast establishment of an equilibrium between adsorbed neptunium(V) on the mineral surface and neptunium in solution.

The fast desorption kinetics could also be observed in ATR-FT IR investigations, where a complete removal of the Np(V) sorption complex characterized by an adsorption band at 790 cm^{-1} was observed. Surface complexation modelling of Np(V) sorption on montmorillonite using the bidentate inner-sphere complex as starting point for the fitting, points toward the formation of both outer-sphere and inner-sphere complexes on the montmorillonite surface in the neutral to alkaline pH range. The outer-sphere complex could not be detected in spectroscopic investigations mainly due to the high pH value of 10 where the outer-sphere complex no longer prevails. The inner-sphere complex was slightly overestimated in modelling pointing towards the presence of some soluble Np(V) complex that could not be resolved in the present study. The presence of carbonates and the formation of soluble Np(V)-carbonato complexes, however, could be ruled out in leaching studies of the montmorillonite suspensions.

4.0 Outcome towards WP1

The work in BELBaR has increased our understanding of bentonite colloid effects on radionuclide transport. It has shown that radionuclides bound by bentonite colloids may be released slowly. In this state, they are bound 'non-exchangeably'. The extent of the effect depends upon the chemistry of the radionuclide. Tri- and tetravelent f-block elements seen to be prone to slow dissociation, with the tetravelent elements able to show slower dissociation than the other species. Actinyl species appear more weakly bound, but may still dissociate slowly. Mono-valent and divalent cations show a rather fast dissociation kinetic with the exception of Cs, where the geological origin of the clay mineral triggering the frayed edge sites is determining the reversibility of sorption. The first order dissociation rate constants found in the literature for colloid dissociation have been significantly enlarged through the BELBaR project and already published values have been to a large extent reconfirmed.
Generally, there are a number of mechanisms that could be responsible for the slow dissociation.

(1) Slow disociation of a surface complex.

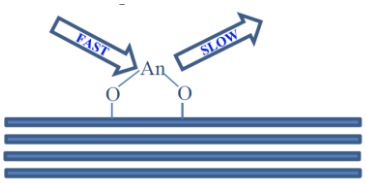

The radionuclides could bind at a surface site from which dissociation is slow. In this case,

the dissociation kinetics would be expected to depend upon the radionuclide chemistry. However, if this is the case, then not all surface complexes show this behaviour, because not all of the loading is bound non-exchangeably.

(2) Slow disociation of a surface precipitate.

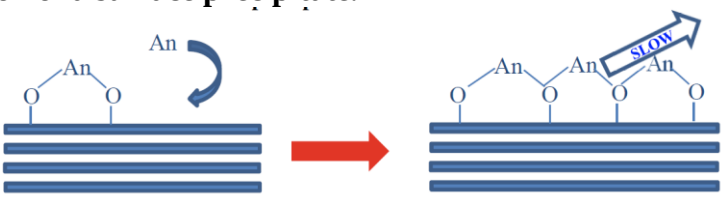

The radionuclides could form a surface precipitate, probably following surface complex formation. Dissolution of this precipitate could be slow. As for surface complexation, the kinetics might be expected to depend upon radionuclide chemistry. Any surface precipitation must take place at very low concentration given that slow dissociation was observed for experiments with very low radionuclide concentrations.

(3) Diffusion in and out of an interlayer.

Radionuclides could enter the clay interlayer from the solution. When a stronger sink becomes available, the radionuclides could then diffuse slowly from the interlayer.

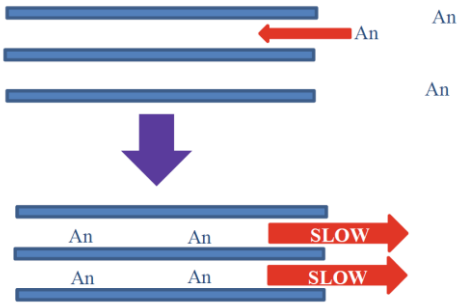

(4) Colloid aggregation.

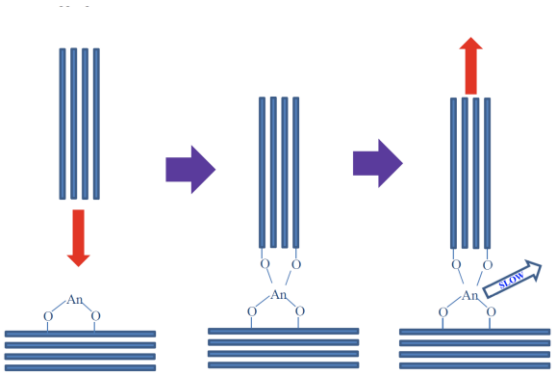

A radionuclide could be bound to a clay colloid in a state that is initially exchangeable.

However, colloidal aggregation could 'trap' the radionuclide in a state where it is 'hidden' from the solution and unavailable for instantaneous reaction. The release from this state could be slow, and might require the dissociation of the aggregate.

Whatever the mechanism, the importance of bentonite colloids in the transport of radionuclides depends on their ability to bind radionuclides 'non-exchangeably'. Mori et al developed the so called 'Colloid Ladder' (Möri et al 2003). An adapted version is shown in Figure 17. The original final criterion in the Colloid Ladder was 'is uptake irreversible?'. However, it has become clear that slow dissociation short of irreversibility can promote transport. Radionuclides will be transported provided that the time required for them to dissociate from the colloid is of the same order or greater than the transport residence time.
Hence, it is not possible to give a single, definitive answer to the question (*Is the assumption of reversible, linear sorption of radionuclides onto colloids justified?*). Rather, we must use a procedure to assess the importance of colloid kinetics for each situation.
Any radionuclides that are bound reversibly, and so may dissociate instantaneously, are expected to be quickly removed by the available mineral surface binding sites, which will be present in excess. For non- exchangeable bound radionuclides that will not prevent transport.
Since the critical factor is the relative magnitudes of the transport residence time and the dissociation rate, the significance of slow dissociation depends upon the conditions of the transport calculation. Hence, a dissociation rate constant that made a significant difference to radionuclide transport in one case, might be much less important in a different scenario, for example at a slower flow rate. Therefore, a method is required to assess the significance of slow dissociation kinetics.

The transport behaviour of a species controlled by kinetics may be rationalised using Damkohler numbers. In a transport calculation, the important timescale is the residence time, t_{res},

$$t_{res} = \frac{L}{V}$$

where L is the distance over which the transport takes place and V is the linear velocity of the mobile phase. For a system with a first order rate constant that represents the rate determining step for dissociation (k_b), it is possible to calculate the amount of radionuclide that will remain bound to the colloid relatively easily, since it will depend only on the rate constant and the time available for dissociation (t_{res}).
Figure 18 shows the dissociation of radionuclides from colloids as a function of residence time: if the time is expressed in units of $1/k_b$, then the plot may be applied to any system. This is the basis of the Damkohler approach. The dimensionless Damkohler number for a metal ion (radionuclide) in the non-exchangeable fraction, D_M, is defined by,

$$D_M = \frac{L}{V} k_b = t_{res} . k_b$$

Systems with the same values of D_M will show analogous behaviour.

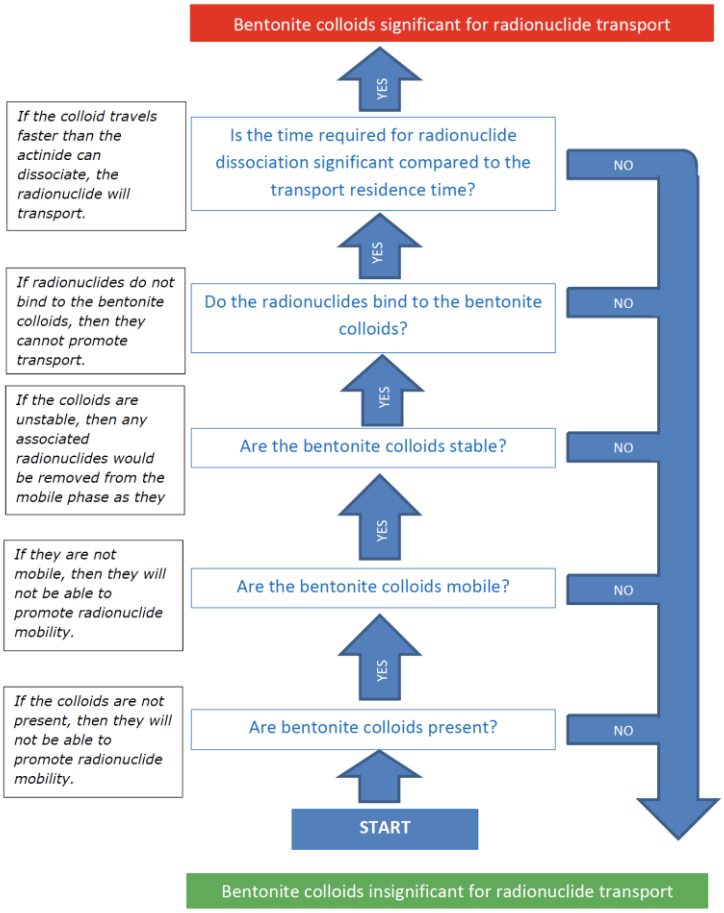

Figure 17: ***The amended colloid ladder taking into account the results of BELBaR.***

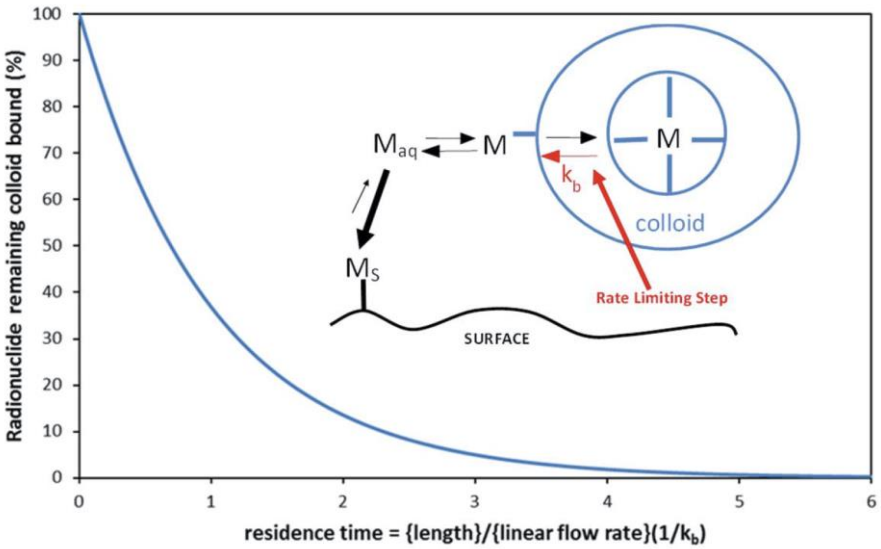

Figure 18: ***Amount of radionuclide remaining colloid bound as a function of residence time, expressed as the reciprocal of the first order dissociation rate constant for a simplified colloid system with a rate limiting step for dissociation of radionuclides (M) from the colloid to allow immobilisation on the solid surface (MS) via the free form (M_{aq}).***

For a given system of colloid and radionuclide, there will be three classes of transport calculation:

1. **Large D_M**: Those where the dissociation is sufficiently fast and/or the transport time sufficiently long that dissociation may be simulated with an equilibrium constant (high k_b and/or high t_{res}).

2. **Low D_M**: Those where the dissociation is sufficiently slow or the residence time sufficiently short that effectively dissociation does not take place (low k_b and/or low t_{res}).

3. **Intermediate D_M**: Those that can only accurately be described by the use of rate equations (intermediate k_b and/or t_{res}).

Given that all systems with the same D_M behave in the same way, we may use it to:

judge the impact of dissociation kinetics;

assign a system to classes 1 – 3;

and, hence judge when it is necessary to include kinetics explicitly in transport calculations.

As the value of D_M decreases, the non- exchangeable bound metal tends towards the behaviour of a conservative tracer (Class 2). In this case, virtually no metal ion leaves the non- exchangeable fraction in the time of the calculation. Therefore, the reaction that connects the exchangeable and non-exchangeable may be removed from the calculation and the two fractions are treated as independent species. The advantage of this approach is that it is inherently conservative.

At high D_M, an equilibrium approximation is possible, although this will tend to underestimate migration, the error decreasing with increasing D_M.

For bentonite colloids, there appears to be a single dissociation rate constant, whilst for HS there are multiple values. In that case, an assessment might be required for each rate constant.

Processes that retard the colloids can have a disproportionate effect on radionuclide transport, since it has the effect of increasing the residence time, allowing more radionuclide to dissociate than would otherwise be expected. This complicates calculations of transport, not least because colloid desorption could be slow. In this case, the radionuclide dissociation and the desorption kinetics are coupled. However, in systems where the interaction of the colloid with the surface may be treated as an equilibrium, an adapted Damkohler number may be used,

$$D_M^{eff} = \frac{k_b}{V} L\,(1 + K_C)$$

where K_C is the equilibrium distribution coefficient for colloid sorption.

5.0 References

Albarran, N., Missana, T., Garcia-Gutierrez, M., Alonso, U. and Mingarro, M., 2011. Strontium migration in a crystalline medium: effects of the presence of bentonite colloids. Journal of Contaminant Hydrology, 122(1-4): 76-85.

Albarran, N.; Missana, T.; Alonso, U.; Garcia-Gutierrez, M.; Lopez, T., Analysis of latex, gold and smectite colloid transport and retention in artificial fractures in crystalline rock. Colloids Surf. A 2013, 435, 115-126.

Alonso, U., Missana, T., Patelli, A., Rigato, V. and Ravagnan., J., 2003. RBS and mPIXE analysis of uranium diffusion from the bentonite to the rock matrix in a deep geological waste disposal. Nuclear Instruments and Methods in Physics Research B, 207(2): 195-204.

Alonso, U., Missana, T., Patelli, A., Rigato, V. and Ravagnan, J., 2007. Colloid diffusion in crystalline rock: An experimental methodology to measure diffusion coefficients and evaluate colloid size dependence. Earth and Planetary Science Letters, 259(3-4): 372-383.

Alonso, U. et al., 2009. Quantification of Au nanoparticles retention on a heterogeneous rock surface. Colloids and Surfaces A: Physicochemical and Engineering Aspects, 347: 230-238.

Alonso, U., Mayordomo, N., and Missana, T. (2016). Cadmium adsorption onto alumina nanoparticles for their use in geochemical barrier for contaminant migration. CIEMAT report , Madrid (Spain). In press.

Bouby, M., Geckeis, H., Lutzenkirchen, J., Mihai, S., Schafer, T. (2011). Interaction of bentonite colloids with Cs, Eu, Th and U in presence of humic acid: A flow field-flow fractionation study, Geochimica et Cosmochimica Acta, 75, 3866–3880.

Bryan, N.D., Abrahamsen, L., Evans, N., Warwick, P., Buckau, G., Weng L.P., and Van Riemsdijk, W.H. (2012) The effects of humic substances on the transport of radionuclides: Recent improvements in the prediction of behaviour and the understanding of mechanisms. Applied Geochemistry 27, 378-389.

Comans R.N.J., (1987), Adsorption, desorption and isotopic exchange of cadmium on illite: evidence for complete reversibility. Water Research 21, 1573–1576.

Darbha, G., T. Schaefer, and J. Luetzenkirchen, 2015 (in preparation), Quantification of interaction forces between clay edge sites and mineral surfaces by colloid probe technique: Environmental Science & Technology.

Darbha, G. K., C. Fischer, J. Luetzenkirchen, and T. Schafer, 2012a, Site-specific retention of colloids at rough rock surfaces: Environmental Science & Technology, v. 46, p. 9378-87.

Darbha, G. K., C. Fischer, A. Michler, J. Luetzenkirchen, T. Schafer, F. Heberling, and D. Schild, 2012b, Deposition of Latex Colloids at Rough Mineral Surfaces: An Analogue Study Using Nanopatterned Surfaces: Langmuir, v. 28, p. 6606-6617.

Geckeis, H., 2008. Colloid influence on the radionuclide migration from a nuclear waste repository Geological Society, London, Special Publications 2004, 236:529-543;. Geological Society, London, Special Publications., 236: 529-543.

Huertas, F. et al., 2000. Full scale engineered barriers experiment for a deep geological repository for high-level radioactive waste in crystalline host rock. EC Final REPORT EUR 19147, EC Final REPORT EUR 19147.

James, S.C. and Chrysikopoulos, C.V., 1999. Transport of polydispersed colloid suspensions

in a single fracture. Water Resources Research, 35(3): 707-718.
Kosakowsky, G., 2004. Anomalous transport of colloids and solutes in a shear zone. Journal of Contaminant Hydrology, 72(1-4): 23-46.
Leskinen, A. et al., 2007. Determination of granites' mineral specific porosities by PMMA method and FESEM/EDAX. In Scientific Basis for Nuclear Waste Management XXX, edited by D.S. Dunn, C. Poinssot, B. Beg. Mater. Res. Soc. Symp. Proc. 985, 0985-NN11-20,Warrendale, PA., Scientific Basis for Nuclear Waste Management. Materials Research Society, Boston, USA.
Miller, W., Alexander, R., Chaoman, N., McKinley, J., and Smellie, J. (1994). Natural analogue studies in the geological disposal of radioactive waste. Studies in Environmental Science 57.
Mayordomo, N., Alonso, U., Missana, T., Benedicto, A., Garcia-Gutierrez, M. (2014). Addition of Al2O3 nanoparticles to bentobnite: effects on surface charge and Cd soprtion properties. Mater. Res. Soc. Symp, Proc. Vol 1665.
Missana, T., Garcia-Gutierrez, M., and Alonso, U. (2004). Kinetics and irreversibility of cesium and uranium sorption onto bentonite colloids in a deep granitic environment. Applied Clay Science 26, 137-150.
Missana, T., Alonso, U., Albarran, N., Garcia-Gutierrez, M. and Cormenzana, J.-L., 2011. Analysis of colloids erosion from the bentonite barrier of a high level radioactive waste repository and implications in safety assessment. Physics and Chemistry of the Earth, 36(17-18): 1607-1615.
Missana, T., Alonso, U., Garcia-Gutierrez, M. and Mingarro, M., 2008a. Role of bentonite colloids on europium and plutonium migration in a granite fracture. Applied Geochemistry, 23(6): 1484-1497.
Missana, T., Garcia-Gutierrez, M., and Alonso, U. (2008b). Sorption of strontium onto illite/smectite mixed clays. Physics and Chemistry of the Earth 33, S156-S162.
Missana, T. , Alonso, U., Garcia-Gutierrez, M., López, T. (2015a) Analysis of bentonite colloid generation in-situ at the FEBEX galley (GTS) global evaluation of experimental data obtained. BELBAR deliverable 2.10 (2015)
Missana, T., Alonso, U., Mayordomo, N., Garcia-Gutierrez, M. (2015b) Cadmium adsorption onto Na-montmorillonite: experimental and modelling study. CIEMAT publication (In press).
Möri, A. et al., 2003. The colloid and radionuclide retardation experiment at the Grimsel Test Site: influence of bentonite colloids on radionuclide migration in fractured rock. Colloids and Surfaces A, 217: 33-47.
Norrfors, K. K.; Marsac, R.; Bouby, M.; Heck, S.; Wold, S.; Lützenkirchen, J.; Schäfer, T., Montmorillonite colloids: II. Colloidal size dependency on radionuclide adsorption. Applied Clay Science, doi:10.1016/j.clay.2016.01.017.
Norrfors, K. K.; Bouby, M.; Heck, S.; Finck, N.; Marsac, R.; Schäfer, T.; Geckeis, H.; Wold, S., Montmorillonite colloids: I. Characterization and stability of dispersions with different size fractions. Appl. Clay Sci. 2015, 114, (0), 179-189.
Powell, K. J., Brown, P. L., Byrne, R. H., Gajda, T., Hefter, G., Leuz, A.-K., Sjöberg, S., and Wanner, H. (2011). Chemical speciation of environmentally significant metals with inorganic ligands. Part 4: The Cd2+, OH–, Cl–, CO32–, SO42–, and PO43– systems (IUPAC Technical Report). Pure and Applied Chemistry 83, 1163–1214.
Romanchuk Anna, Y.; Kalmykov Stepan, N.; Aliev Ramiz, A., Plutonium sorption onto

hematite colloids at femto- and nanomolar concentrations. In Radiochimica Acta International journal for chemical aspects of nuclear science and technology, 2011; Vol. 99, p 137.
Sabodina, M. N.; Kalmykov, S. N.; Sapozhnikov, Y. A.; Zakharova, E. V., Neptunium, plutonium and Cs-137 sorption by bentonite clays and their speciation in pore waters. Journal of Radioanalytical and Nuclear Chemistry 2006, 270, (2), 349-355.
Schaefer, T. et al., 2012. Nanoparticles and their influence on radionuclide mobility in deep geological formations. Applied Geochemistry, 27(2): 390-403.
Schäfer, T., Geckeis, H., Bouby, M. and Fanghänel, T., 2004. U, Th, Eu and colloid mobility in a granite fracture under near-natural flow conditions. Radiochimica Acta, 92(9-11).
SKB Sorption of prioritized elements on montmorillonite colloids and their potential to transport radionuclides, Technical report TR-10-20; Technical report TR-05-20; Svensk Kärnbränslehantering AB: Stockholm, Sweden, 2010; p 43.
Stumm, W. (1992). "Chemistry of the solid-water interface. J. Wiley and Sons N.Y.
Stoll, M., G. Darbha, F. Huber, E. Schill, and T. Schaefer, 2015 (in preparation), Impact of gravity and particle size on monodisperse polystyrene particles in an artificial fracture flow cell: Langmuir.
Zavarin, M.; Powell, B. A.; Bourbin, M.; Zhao, P.; Kersting, A. B., Np(V) and Pu(V) Ion Exchange and Surface-Mediated Reduction Mechanisms on Montmorillonite. Environ. Sci. Technol. 2012, 46, (5), 2692-2698.
Zirino, A., and Yamamoto, S. (1972). A pH-dependent model for teh chemical speciation of copper, zinc, cadmium, and lead in seawater. Limnology and Oceanography 17, 661-671.

ANNEX

Delivered as a Excel Spreadsheet

Summary tables of individual partner data provided within CP BELBaR.

Batch SORPTION					
Colloidal Phase					
Element					
Oxidation state					
Speciation (species calculated or spectroscopically identified)					
Concentration					
pH					
V/m					
Contact duration					
atmosphere (e.g. Ar +/- CO2…)					
water type					
distribution coefficient					
sorption kinetic (rate; h-1)					
Desorption studies					
Colloid associated element concentration					
pH					
column migration/ batch type					
concurrence ligand					
desorption time					
reversibility achieved					
reversibility possible to detect based on analytical detection limit					
desorption rate (h-1)					

Publication associated with the dataset provided (if any):